



ASN

Autorité de
sûreté nucléaire
et de radioprotection

RÉPUBLIQUE FRANÇAISE

UPDATE OF THE NUCLEAR CRITICALITY SLIDE-RULE

TECHNICAL BASIS

Rapport d'étude N° 2025-00084

DIRECTION DE LA RECHERCHE EN SÛRETÉ

FICHE DESCRIPTIVE
DESCRIPTION SHEET

Title	<i>Update of the nuclear criticality Slide Rule</i>
Subtitle	<i>Technical Basis</i>
Auteur(s)/Author(s)	J. HERTH
Élément d'imputation	01/08/02/08

HISTORIQUE DES MODIFICATIONS
CHANGE HISTORY

Indice de révision <i>Revision</i>	Date	Rédacteur <i>Author</i>	Pages ou paragraphes modifiés <i>Pages or paragraphs changed</i>	Nature des modifications <i>Nature of the changes</i>
0	06/05/19	M. TROISNE	/	Document creation (report IRSN/2019-00266)
1	17/03/25	J. HERTH	§4.3, §4.4, §5.3	Adding results from uranium configuration (sensitivity studies) and plutonium configuration (delayed fission gamma)

Rédacteur(s) <i>(Author(s))</i>	Vérificateur(s) <i>(Reviewer(s))</i>	Approbation (<i>approval</i>)		
		Chef de service <i>(Head of department)</i> - Chef de projet <i>(Project leader)</i>	Chargé de projet majeur <i>(Top project leader)</i>	Responsable d'axe programme <i>(Program leader)</i>
Nom/ <i>Name</i>	J. HERTH	A. BARDELAY	S. PIGNET	J. FLEUROT
Date	17/03/2025			
Visa				

RÉSUMÉ

Mots clés : accident de criticité, slide-rule, dosimétrie

Dans le cadre de la collaboration entre l'ASNR (anciennement IRSN) et le Nuclear Safety Criticality Program (NCSP) de l'US-DoE, une action de révision des calculs réflexes de doses en situation d'urgence résultant d'un accident de criticité a été initiée en 2015. Cette action consiste à réaliser des calculs de dosimétrie par différents partenaires ASNR (FR), AWE (UK), ORNL (USA) et LLNL (USA). Les doses en cas d'accident de criticité sont évaluées, en phase réflexe, via une "slide rule". Cette règle à calcul, publiée il y a plus de 20 ans, donne des ordres de grandeur telles que le nombre de fissions, les doses (neutron et gamma), utiles aux autorités publiques et aux équipes de secours.

Ce rapport présente :

- la mise en place d'une méthode de calculs de dose et son application aux cinq milieux fissiles considérés dans les « Slide-Rule » d'origine (configurations uranium);
- une extension des configurations originales aux systèmes plutonium ;
- la comparaison des résultats obtenus avec différents codes Monte-Carlo utilisés par les différents partenaires (MCNP, SCALE et COG) ;
- des comparaisons entre différents facteurs de conversion flux-dose.

SUMMARY

Key-words: nuclear criticality accident, slide-rule, dosimetry

ASNR (formerly IRSN, FR), AWE (UK), LLNL (USA) and ORNL (USA) began a long-term collaboration effort in 2015 to update the Nuclear Criticality Slide Rule for the emergency response to a nuclear criticality accident. This document published more than 20 years ago, gives order of magnitude estimates of key parameters, such as number of fissions and doses (neutron and gamma), useful for emergency response teams and public authorities.

This report gives:

- calculation scheme and its application to the five fissile media considered in the "Slide Rule";
- an extension of the original "Slide Rule" configurations to plutonium systems;
- comparisons between Monte-Carlo codes used by the participants (such as MCNP, SCALE and COG);comparisons between different flux-to-dose conversion factors.

TABLE OF CONTENTS

1. INTRODUCTION.....	8
2. OBJECTIVES OF THIS UPDATE.....	9
3. CODES AND METHODS USED	10
3.1. ASNR.....	10
3.2. ORNL.....	10
3.3. LLNL.....	11
4. URANIUM CONFIGURATIONS	12
4.1. Model description	12
4.2. Results	13
4.2.1. Prompt calculations.....	13
4.2.2. Delayed gamma doses	17
4.3. Sensitivity studies	22
4.3.1. Air composition	22
4.3.2. Ground composition and dimensions	22
4.3.3. Skyshine.....	23
4.4. Shielded configurations.....	24
4.4.1. Water	24
4.4.2. Steel.....	25
4.4.3. Lead	26
4.4.4. Concrete	27
4.4.5. Code-to-code comparison.....	28
4.4.6. Impact of screen position.....	30
5. PLUTONIUM CONFIGURATIONS.....	32
5.1. Model description	32
5.2. Results	32
5.2.1. Bare sphere calculations	32
5.2.2. Bare cylinder calculations.....	36
5.2.3. Reflected sphere calculations	37
5.3. Delayed fission gamma (DFG).....	38
5.3.1. Configuration overview and assumptions.....	38
5.3.2. DFG dose rates results.....	39
5.3.3. Code-to-code comparison	40

6. FLUX-TO-DOSE CONVERSION FACTORS	42
6.1. Energy mesh for flux calculations	42
6.2. Application of a flux-to-dose conversions factors.....	43
6.2.1. Comparisons for the neutron doses.....	43
6.2.2. Comparisons for the gamma doses.....	44
7. CONCLUSIONS AND PERSPECTIVES	46

TABLES AND FIGURES

List of Figures

Figure 1. « 1997 Slide Rule » for the uranyl nitrate solution.	8
Figure 2. X-Z elevation view of the initial configuration	13
Figure 3. X-Y plan view of the initial configuration.	13
Figure 4. Comparison of prompt doses for uranium dioxide.	14
Figure 5. Comparison of prompt doses for enriched uranyl nitrate.	14
Figure 6. Comparison of prompt doses for enriched uranium metal	14
Figure 7. Code-to-code dose ratio (with 2σ error bars) for uranium dioxide	15
Figure 8. Code-to-code dose ratio (with 2σ error bars) for uranyl nitrate	15
Figure 9. Code-to-code dose ratio (with 2σ error bars) for uranium metal	15
Figure 10. Comparison of delayed gamma dose rates for uranyl fluoride 1 s after the criticality accident	17
Figure 11. Comparison of delayed gamma dose rates for uranyl fluoride 1 min after the criticality accident	17
Figure 12. Comparison of delayed gamma dose rates for uranyl fluoride 10 min after the criticality accident	18
Figure 13. Comparison of delayed gamma dose rates for uranyl fluoride 100 min after the criticality accident	18
Figure 14. Comparison of delayed gamma dose rates for uranyl fluoride 1000 min after the criticality accident	18
Figure 15. Delayed gamma dose rates for uranyl nitrate vs UO_2 , 10 min after the criticality accident	19
Figure 16. Intensity of delayed gamma as a function of the decay time for the uranyl fluoride	20
Figure 17. MCNP/SCALE delayed gamma dose rate ratio (with 2σ error bars) for enriched uranium metal	20
Figure 18. COG/SCALE delayed gamma dose rate ratio (with 2σ error bars) for enriched uranium metal	20
Figure 19. MCNP/SCALE delayed gamma dose rate ratio (with 2σ error bars) for uranyl fluoride	21
Figure 20. COG/SCALE delayed gamma dose rate ratio (with 2σ error bars) for uranyl fluoride	21
Figure 21. Code-to code delayed gamma dose rate ratio for all cases at 10 meters from the criticality accident	21
Figure 22. Ratio of prompt doses calculated with air humidity to the prompt doses calculated with dry air.	22
Figure 23. Ratio of prompt doses for 50 cm dry soil to those for 30.48 cm 'concrete' soil.	23
Figure 24. Ratio of prompt doses for a 10 m sky height to those for a 1.5 km sky height.	23
Figure 25. Case 1 – Water – Ratio of prompt doses with shield to without shield.	25
Figure 26. Case 4 – Water – Ratio of prompt doses with shield to without shield.	25
Figure 27. Case 1 – SS304 – Ratio of prompt doses with shield to without shield.	26
Figure 28. Case 4 – SS304 – Ratio of prompt doses with shield to without shield.	26
Figure 29. Case 1 – Lead – Ratio of prompt doses with shield to without shield.	27
Figure 30. Case 4 – Lead – Ratio of prompt doses with shield to without shield.	27

Figure 31. Case 1 – Concrete – Ratio of prompt doses with shield to without shield.	28
Figure 32. Case 4 – Concrete – Ratio of prompt doses with shield to without shield.	28
Figure 33. Case 1 – Concrete – SCALE-to-MCNP doses ratio.	29
Figure 34. Case 4 – Concrete – SCALE-to-MCNP doses ratio.	29
Figure 35. Case 1 – Concrete – COG-to-MCNP doses ratio.	29
Figure 36. Case 4 – Concrete – COG-to-MCNP doses ratio.	30
Figure 37. Case 4 – N – Concrete (20 cm) – Ratio of neutron prompt doses with and without screen for six screen positions.	31
Figure 38. Neutron prompt doses for bare plutonium sphere calculated with MCNP	33
Figure 39. Gamma prompt doses for bare plutonium sphere calculated with MCNP	33
Figure 40. Neutron/gamma prompt dose ratio for bare plutonium sphere calculated with MCNP	34
Figure 41. Code to code comparison for the bare plutonium sphere	35
Figure 42. Henderson/ANSI-HPS N13.3 dose ratios for bare plutonium sphere (MCNP)	35
Figure 43. Henderson/ANSI-HPS N13.3 flux-to-dose conversion factors	36
Figure 44. Bare sphere prompt doses using Henderson flux-to-dose conversion factors (MCNP)	36
Figure 45. Bare cylinder/sphere dose ratios (SCALE) for H/Pu=0 (left) and H/Pu=2000 (right)	37
Figure 46. Reflected/bare sphere dose ratios (COG) for H/Pu=0 (left) and H/Pu=2000 (right)	38
Figure 47. Overview of the ASNR (FISPACT-MCNP) results obtained with HPS N13.3 conversion factor	39
Figure 48 Comparison of DFG dose rates between Pu and U metal (H/X =0).	40
Figure 49 Comparison of ASNR DFG dose rates from two depletion codes with LLNL and ORNL results (d ≤ 300 m)	40
Figure 50 DFG dose rate code-to-code comparison: ORNL vs LLNL results (d ≤ 300 m).	41

List of Tables

Table 1. Upper bounds in MeV of the neutron energy mesh (from left to right and top to bottom)	42
Table 2. Upper bounds in MeV of the gamma energy mesh (from left to right and top to bottom)	43
Table 3. Designations of the different flux-to-dose conversion factors	44
Table 4. Ratios and relative errors of the neutron prompt dose calculated using the energy mesh with a 'two-step' calculation and a direct calculation	44
Table 5. Ratios and relative errors of the gamma prompt dose calculated using the energy mesh with a 'two-step' calculation and a direct calculation	44

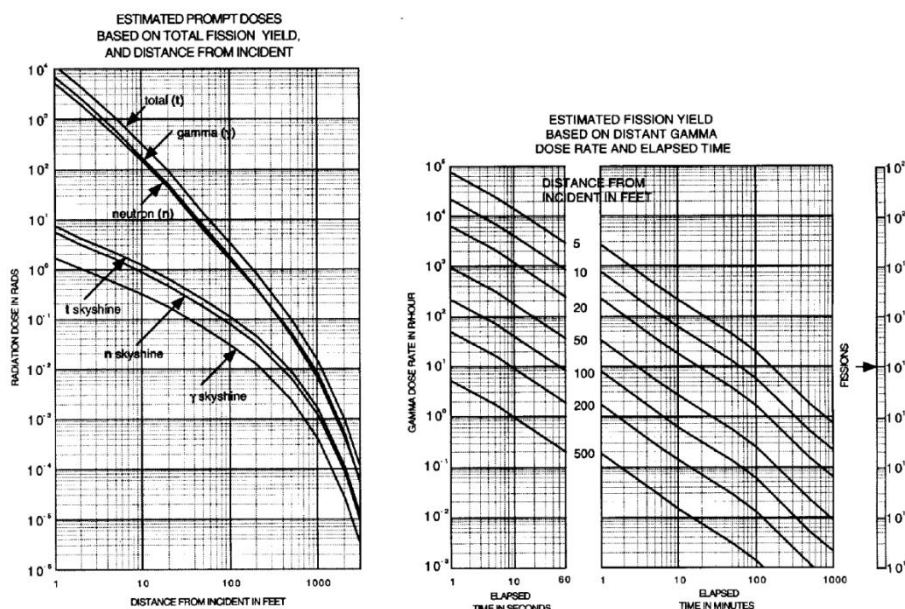
1. INTRODUCTION

In 1997 Oak Ridge National Laboratory published the report "An Updated Nuclear Criticality Slide Rule" [1]-[2] as a tool for emergency response to a nuclear criticality accident. A similar document was produced by the Institut de Radioprotection et de Sécurité Nucléaire (IRSN) in 2000 [3]. According to [1], this kind of document "permits continued updating of information during the evolution of emergency response, including exposure information about victims, estimates of potential exposures to emergency response re-entry personnel, estimates of future radiation field magnitudes, and number of fissions (fission yield) estimate" without precisely knowing the initial conditions leading to the criticality accident.

This document gives order of magnitude estimates of key parameters, useful for emergency response teams and public authorities. In practice, the "Slide Rule" provides estimates of the following information based upon variable times and distances from the accident:

- the magnitude of the number of fissions based on personnel or field radiation measurements,
- prompt neutron- and gamma-dose at variable unshielded distances from the accident,
- the skyshine component of the prompt dose,
- time-integrated total radiation dose estimates,
- accumulated one-minute gamma radiation dose as a function of time after the accident, and
- dose-reduction factors for variable thicknesses of steel, concrete and water.

The 1997 Slide Rule provides estimates for five unreflected spherical uranium systems that give general characteristics of operations typical of facilities licensed by the US Nuclear Regulatory Commission. An example of this Slide Rule is presented in Figure 1.



Slide 1 Solution of $\text{U}(93.2)\text{O}_2(\text{NO}_3)_2$ @ $\text{H}^{235}\text{U} = 500$

Figure 1. « 1997 Slide Rule » for the uranyl nitrate solution.

Several laboratories have determined the need to review, update, and expand the contents of the 1997 Slide Rule. In particular, the conversion factors used to provide doses (Henderson flux-to-dose factors) are outdated, so additional conversion factors are used. Also, new configurations need to be added, especially plutonium systems. This document combines and completes the work presented in [4] and [5].

2. OBJECTIVES OF THIS UPDATE

A long term collaboration effort between ASNR¹ (formerly IRSN, France), AWE (UK), LLNL (USA), and ORNL (USA) in the framework of the U.S. DoE Nuclear Criticality Safety Program (NCSP) [6], began in order to update the Slide Rule with modern tools and add new configurations, taking into account the experience of several laboratories in using the 1997 Slide Rule. As a result, the complete work is envisioned to spread over many years and to be divided into five phases:

- 1) Recalculation of initial configurations for uranium systems using modern radiation transport tools, with the same configurations and assumptions as the 1997 dose estimations. This includes evaluations of both prompt and delayed doses.
- 2) Perform additional calculations to enhance the quality and quantity of information provided to the Slide Rule users. The goal is not only to deliver a single value but also to present potential variations and the range of applicability of this value. These additional calculations have included:
 - a) The evaluation of new fissile media (e.g., plutonium systems).
 - b) New configurations assessing the impact of source geometry (sphere vs. cylinder) and source reflection (bare vs. steel-reflected sphere).
 - c) Updated flux-to-dose conversion factors (for dosimetry, radiological protection, and instrumentation purposes).
- 3) Sensitivity studies: evaluation of the impact of shielding materials (lead, steel, concrete, water), air humidity, ground composition and thickness, and the skyshine effect on uranium system doses.
- 4) Assessment of delayed gamma dose rates for plutonium systems, caused by the release of fission products.
- 5) Estimation of the total number of fissions during the entire criticality accident, including boiling for water-moderated systems, based on heat energy formulae.
- 6) Advanced sensitivity studies for plutonium systems, replicating the shielding and sensitivity analyses performed for uranium systems, while incorporating additional shield position effects relative to the source

Based on the previous work, the final task will be the development of a Slide Rule "application" for a handheld device (e.g. smartphone).

At the end, this work should improve the expertise for the real time response to a criticality accident in order to minimize the consequences of such an accident. In addition, this work will provide the opportunity to suggest experiments allowing the complete or partial validation of the tool results (benchmarking effort).

Another consequence of this collaborative effort might be the creation of "computational benchmarks" in order to test and verify the various variance reduction methods and to establish best practices when dealing with this kind of problem.

The first phase was to redo with modern radiation transport tools, for the same configurations and assumptions, the calculations performed initially for the 1997 estimation of the doses. This effort is presented in chapter 4. Moreover, chapter 5 presents and discusses results for new configurations (phase 2) including plutonium systems, calculated by modern 3D radiation transport codes, MCNP, SCALE and COG. Finally, chapter 6 presents studies on the impact of the flux-to-dose conversion factors.

¹ IRSN became ASNR (Autorité de Sûreté Nucléaire et de Radioprotection) on January 1, 2025

3. CODES AND METHODS USED

This section describes the different codes and computational methods used by the laboratories contributing to this work.

3.1. ASNR

MCNP 6 [7], a general-purpose Monte Carlo radiation transport code developed by Los Alamos National Laboratory (LANL), was used with the continuous energy ENDF/B-VII.1 cross-section library for the particle transport involved in both prompt and delayed gamma dose computations. Additional information regarding this kind of calculations with MCNP might be found in references [8] and [9]. Both calculations followed a two-step process, detailed as follows.

Prompt dose

1. Source term

A static calculation (KCODE mode) was conducted to determine the spatial distribution of fission neutron production within the fissile sphere. The production was calculated using a Watt spectrum for energy distribution and tallied in 20 equal volume meshes, either as spheres (SMESH) or cylinders (CMESH).

2. Dose calculation

The fission reaction rates from step 1 were used as a fixed source (SDEF mode) of fission neutrons. Prompt gamma and neutron doses were determined in the same calculation, with gammas being produced by the neutron interactions inside the fissile sphere. In this step, the fission neutron production was turned off (treated as absorption), but all gammas, including fission gammas, are produced (NONU = 0)

Delayed fission-product gamma dose

1. Source term

To produce the delayed gamma source, a sequence of modules (KENO, MONACO, COUPLE, and ORIGEN) from the SCALE 6.1.2 [11] package was used to calculate spectra and intensities².

Additionally, for comparative purposes, the FISPACT-II 5.0 [12] inventory and source-term code was used independently of SCALE to generate fission product gamma sources.

2. Dose calculation

The spatial distributions of the prompt fission neutron mesh source and the delayed gamma mesh source were kept consistent. An MCNP F4 tally was used to estimate cell fluxes, paired with an energy multiplier (EM card) to score the delayed gamma dose rates at desired distances.

Variance Reduction

ADVANTG [10], a 3D deterministic code, was used to generate variance reduction parameters and a biased source for the Monte Carlo fixed source calculations. The relative errors were kept as low as reasonably achievable and all but the Pareto slope check among MCNP's 10 statistical checks were passed.

3.2. ORNL

SCALE [11] is a comprehensive modeling and simulation suite developed and maintained by Oak Ridge National Laboratory (ORNL). SCALE 6.2.1 was used with the ENDF/B-VII.1 continuous energy cross section library, utilizing the CAAS analysis capability that couples KENO and MAVRIC/Monaco, similar to the MCNP analysis

² KENO calculates the distribution of fission neutron production inside the fissile sphere. MONACO uses the KENO result and calculates the neutron flux inside the fissile sphere. COUPLE uses the resulting MONACO neutron flux and creates problem dependent flux weighted cross sections to produce reaction rates. ORIGEN uses these reaction rates and performs the depletion and decay of the fissile systems.

methodology. Initially, KENO was run with a Cartesian mesh tally of fission neutron production to capture the asymmetry caused by the ground 1 m below each fissile sphere. Following this, MAVRIC/Monaco used the KENO fission source distribution as a fixed source to generate variance reduction parameters and simulate prompt doses. Region tallies were used in the model to calculate doses at the desired distances by introducing cells that were cylindrical shells in the actual problem geometry, as was done with MCNP. For the prompt dose calculations, total nu-bar was used just like the MCNP calculations.

The delayed gamma source was similarly produced using KENO/MONACO coupled with ORIGEN from the SCALE package that the MCNP calculations used. For the plutonium delayed gamma cases, a very-fine AMPX 1597-group structure (v7.1-1597n) nuclear data library was used from SCALE 6.3. The use of the very-fine group structure allowed for increased accuracy neutron flux and activation source calculations in plutonium spheres, using ORIGEN to generate activation sources dependent on the group structure, with MAVRIC recalculating doses from activation and fission product gammas in a gamma-only simulation.

3.3. LLNL

COG [13] is a full-featured Monte Carlo radiation transport code developed by Lawrence Livermore National Laboratory (LLNL) that provides accurate simulation results to complex shielding, criticality, and activation problems. COG 11.2 was used with ENDF/B-VII.1 cross-section library data.

A feature in COG can generate, track and score track and score delayed fission gamma (DFG) rays born between two given times. Point-wise continuous cross-sections are used in COG and a full range of biasing options are available for speeding up solutions for deep penetration problems.

A direct one-phase criticality/detector calculation method was applied for all neutrons and prompt and delayed gamma ray dose calculations. All neutron and gamma particles are tracked from birth due to fission within the spherical fissile volume to absorption in or leakage from the system in one single, massively parallel, COG supercomputer run with no variance reduction biasing applied. To activate the DFG option, DELAYEDPHOTONS (and associated time interval values) and DGLIB are input in the BASIC and MIX blocks, respectively. A 1 cm high cylindrical boundary-crossing detector was used to score the dose calculations.

4. URANIUM CONFIGURATIONS

The critical uranium systems considered for the initial configuration of the 1997 Slide Rule were:

- Unreflected sphere of 4.95 wt% enriched aqueous uranyl fluoride, $\text{U}(4.95)\text{O}_2\text{F}_2$ and H_2O , solution having a hydrogen-to- ^{235}U ratio of 410 (solution density = 2.16 g/cm³),
- Unreflected sphere of damp 5 wt% enriched uranium dioxide, $\text{U}(5)\text{O}_2$, having a hydrogen-to- ^{235}U ratio of 200,
- Unreflected sphere of 93.2 wt% enriched uranyl nitrate, $\text{U}(93.2)\text{O}_2(\text{NO}_3)_2$ and H_2O , solution having a hydrogen-to- ^{235}U atom ratio of 500 (solution density = 1.075 g/cm³),
- Unreflected sphere of 93.2 wt% enriched uranium sphere (metal density = 18.85 g/cm³),
- Unreflected sphere of damp 93.2 wt% enriched uranium oxide, U_3O_8 plus water, having a hydrogen-to- ^{235}U atom ratio of 10 (uranium oxide density = 4.15 g/cm³).

Neutron and gamma doses were calculated as a function of distance from 1 to 3000 feet (0.3048 to 914.4 m) from the surface of the critical sphere.

4.1. Model description

The geometry for the 1997 Slide Rule models consists of a simple 2-D air-over-ground configuration with the source located at the radial center of a right-circular cylinder. The radius and the height of the air cylinder is 1530 m. The center of the critical assemblies (spheres) are all 1 m above the ground. The ground is modelled as a 30.48 cm (1 ft) layer of concrete. The dimensions of the critical spheres and the composition of all materials can be found in references [1], [2] and [14].

Figure 2 and Figure 3 present the model for these initial calculations. For more clarity, all the information needed to calculate the initial configuration was written in a specific document using a “benchmark format” [14]. Furthermore, a common file naming convention for the various cases has been adopted. The same principle will be used, in the future, for additional configurations. An example is the following:

SR-U-UN-G1-C1-d500-DG10s stands for:

- SR: Slide Rule,
- U: uranium,
- UN: unreflected (no shielding),
- G1: first case with ground (30.48 cm of concrete),
- C1: first case with uranium system³,
- d500: distance of 500 m from the critical sphere,
- DG10s: delayed gamma (after 10 seconds)⁴.

³ C1 is Uranyl fluoride (4.95%); C2 is Damp UO₂ (5%); C3 is Uranyl nitrate solution (93.2%); C4 is U metal (93.2%); C5 is Damp U₃O₈ (93.2%).

⁴ Instead of « DG », « N » and « G » may be used, for respectively prompt neutron and prompt gamma

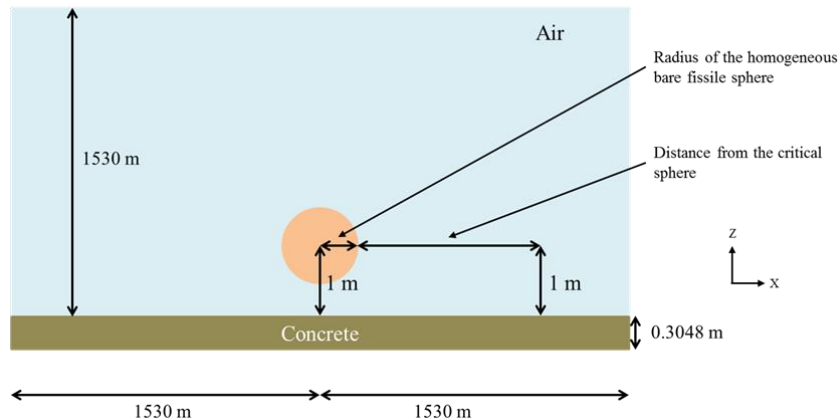


Figure 2. X-Z elevation view of the initial configuration

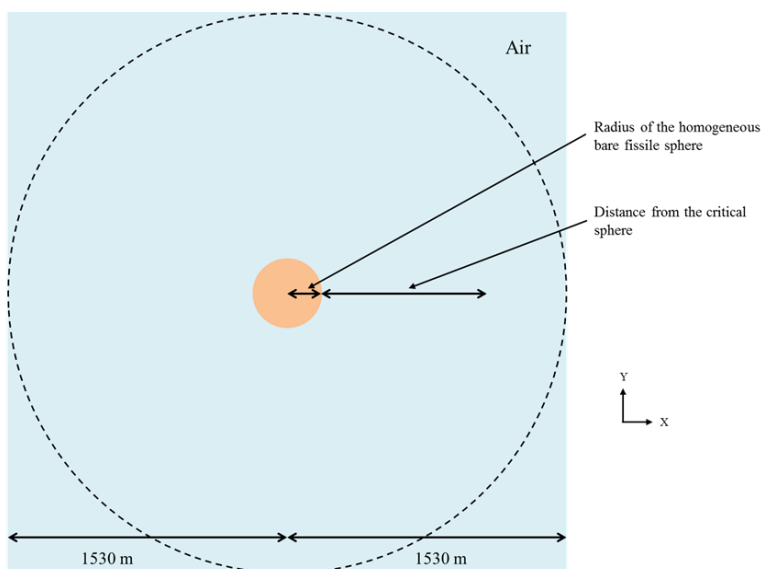


Figure 3. X-Y plan view of the initial configuration.

4.2. Results

This section presents and discusses the simulation results for the cases described in the previous section as well as the comparison with the 1997 Slide Rule. As specified in reference [14], without taking into account the skyshine calculations, at least 900 results are needed to cover all the cases. The laboratories used the various codes and methods presented in chapter 3. Every laboratory used the Henderson flux-to-dose conversion factors [15] in order to compare the results with the 1997 Slide Rule results. The impact of flux-to-doses conversion factors are discussed in chapter 6. Doses are given for 1.E+17 fissions.

4.2.1. Prompt calculations

Prompt dose comparisons are performed between the 1997 Slide Rule and the modern codes. Complete doses results are presented in Appendix 1. Figure 4 to Figure 6 show comparisons for three cases and Figure 7 and Figure 8 are focused on the code-to-code comparison for all cases.

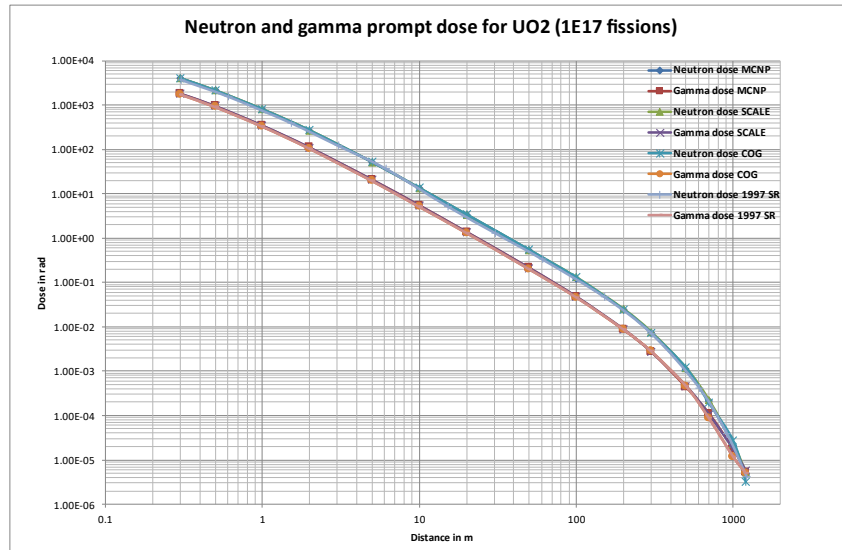


Figure 4. Comparison of prompt doses for uranium dioxide.

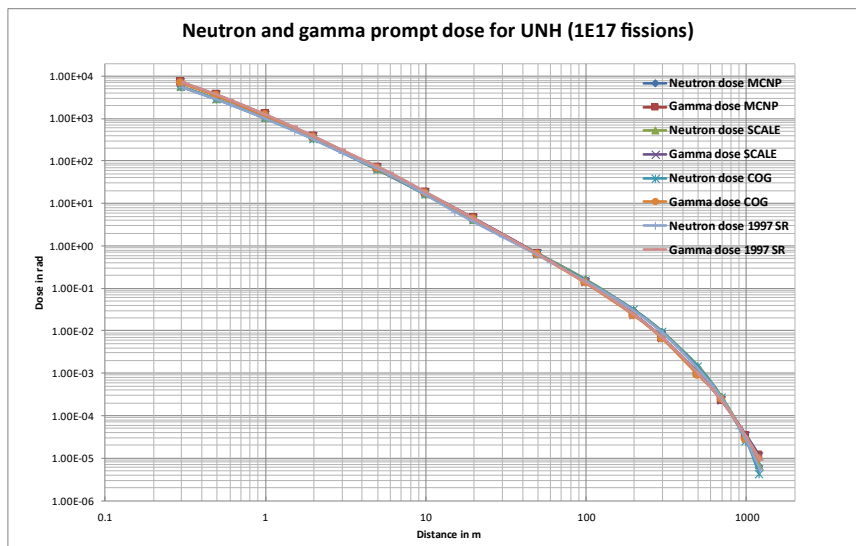


Figure 5. Comparison of prompt doses for enriched uranyl nitrate.

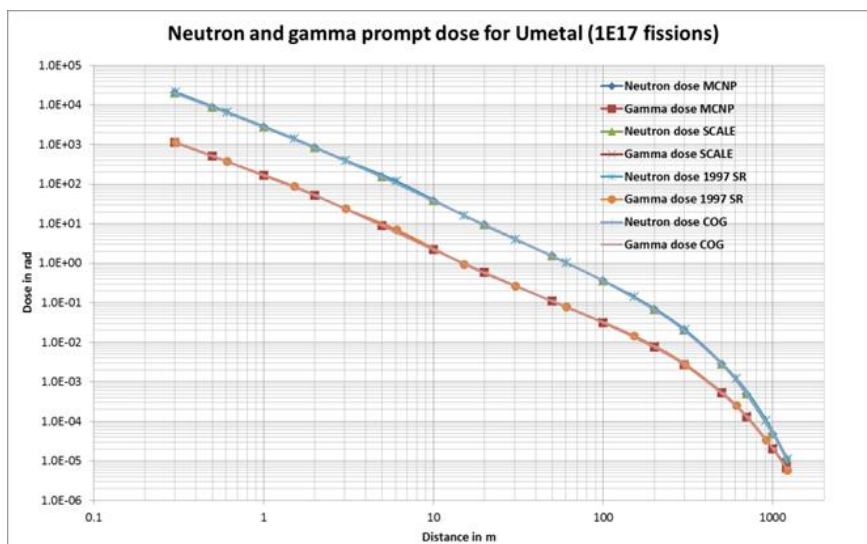


Figure 6. Comparison of prompt doses for enriched uranium metal

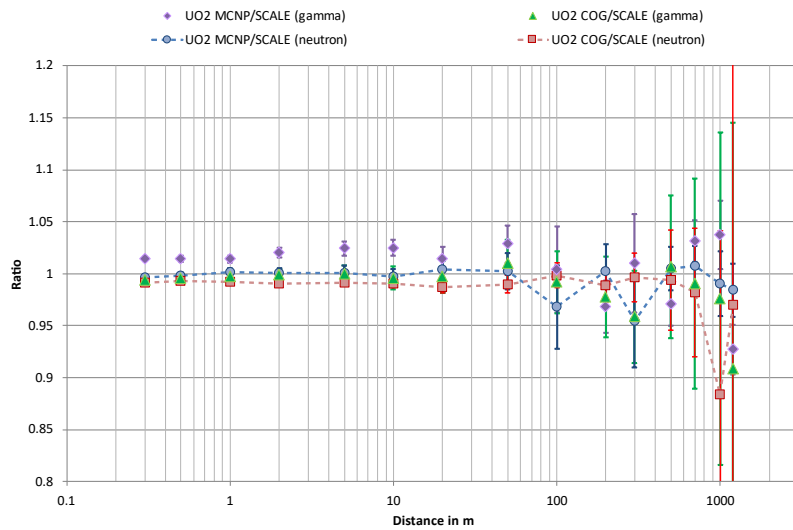


Figure 7. Code-to-code dose ratio (with 2σ error bars) for uranium dioxide

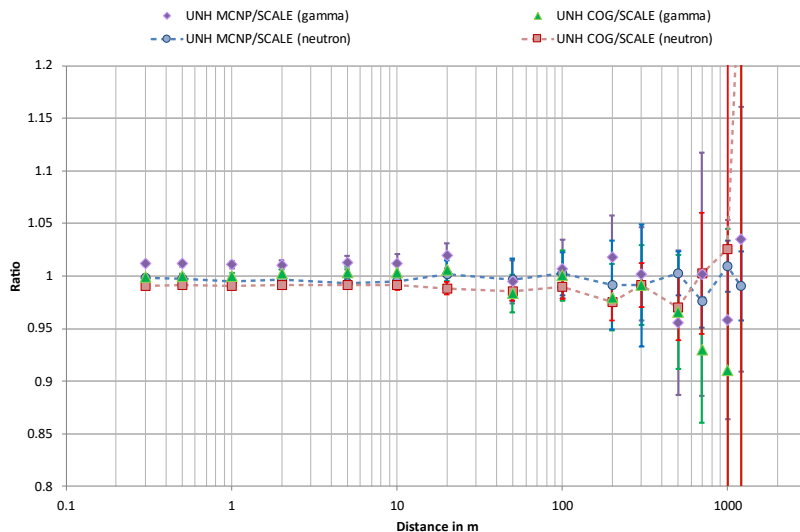


Figure 8. Code-to-code dose ratio (with 2σ error bars) for uranyl nitrate

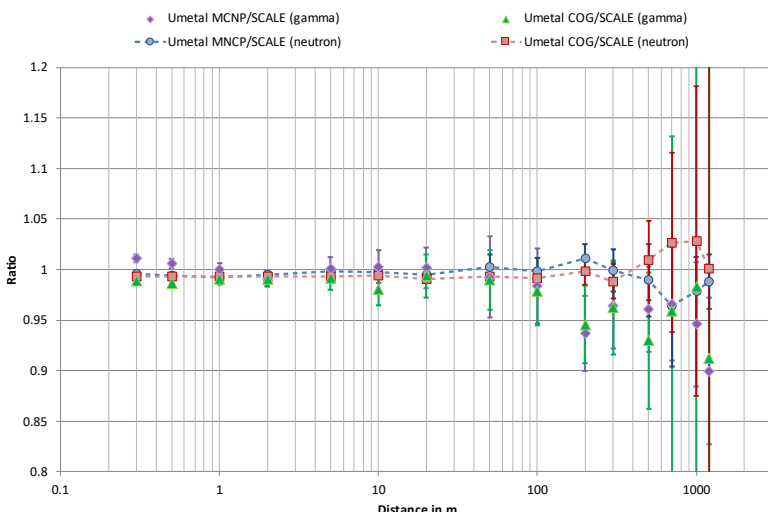


Figure 9. Code-to-code dose ratio (with 2σ error bars) for uranium metal

A good agreement is observed between the 1997 Slide Rule results and the modern codes results for both prompt neutron and gamma doses for all cases. The discrepancies between codes are generally below 5%.

The corresponding relative error (2σ) on the dose ratio between two codes is generally lower than 13% for neutrons (for any distance) and for gammas for distance lower than 300 m. After 300 m, the corresponding relative error on the ratio for gamma increases and can reach 25% for the MCNP/SCALE comparison and 60% for the COG/SCALE comparison.

This discrepancy between codes seems to increase with distance for both neutrons and gamma doses, although the effect is more pronounced for gamma doses. A possible explanation is that the prompt gamma contribution from the uranium sphere decreases with the distance increase. The gammas being produced by neutrons in the concrete and air, far from the uranium sphere, need to be correctly taken into account. This problem requires very good convergence not only for gammas created inside the uranium sphere, but also for neutrons that create gamma (in the ground) near to the detector. These trends are observed consistently across all three codes, suggesting that the discrepancies stem from the complexity of modeling gamma contributions, especially those produced by neutrons interacting with surrounding materials.

One known difference between MCNP and SCALE gamma transport is MCNP's thick target bremsstrahlung model. This model accounts for the electromagnetic cascade of gammas and electrons that produce many low-energy bremsstrahlung gammas. The MCNP thick target bremsstrahlung model accounts for these gammas, and allows users to not perform electron transport for geometries with thick shielding materials⁵. All of the SCALE fixed-source radiation transport codes use gamma production data based on ENDF, which does not include this sort of bremsstrahlung. Regarding COG, whenever an electron-producing photon reaction occurs, COG checks whether the reaction occurred in a region enabled by the user for electron transport. If not, which is the case here, then the electron energy is immediately deposited locally (no bremsstrahlung is transported).

Regarding the calculation of the prompt doses, the results from the modern tool used for this update are consistent. For the initial 2D configuration, the modern 3D tools results confirm the results obtained with the 2D tool used to create the 1997 Slide Rule. The impact of the use of new nuclear data is not visible on the update, with regard to the relative error (generally 5 %). The interest in 3D capabilities will become more important for new configurations that will break the symmetry of the problem.

⁵ The effect of this model could easily be quantified to confirm if it is the cause of the discrepancies.

4.2.2. Delayed gamma doses

Delayed fission-product gamma dose⁶ comparisons are performed between the 1997 Slide Rule and the modern codes. Many decay times are considered in references [1] and [14] (1, 5 and 10 s and 1, 5, 10, 50, 100, 500 and 1 000 min). So, only representative cases are presented hereafter. Figure 10 to Figure 15 show these comparisons. Complete delayed gamma doses results are presented in Appendix 1.

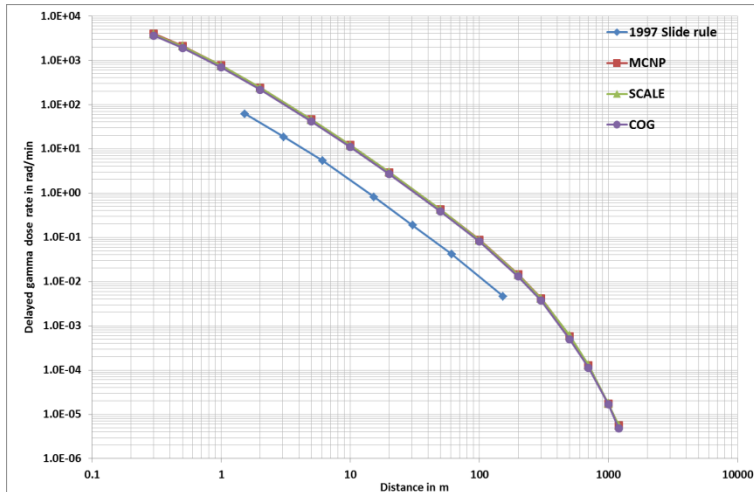


Figure 10. Comparison of delayed gamma dose rates for uranyl fluoride 1 s after the criticality accident

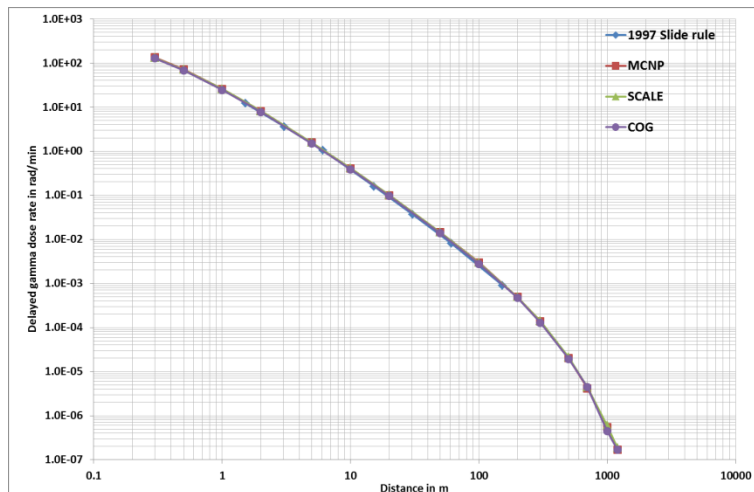


Figure 11. Comparison of delayed gamma dose rates for uranyl fluoride 1 min after the criticality accident

⁶ While delayed neutrons also contribute to the radiation field following a criticality accident, their overall impact on dose is significantly lower compared to prompt neutrons and gamma rays. Moreover, their lower energy and limited biological impact render their contribution negligible for most dose assessments. Consequently, the evaluation of delayed neutron dose was excluded from this analysis.

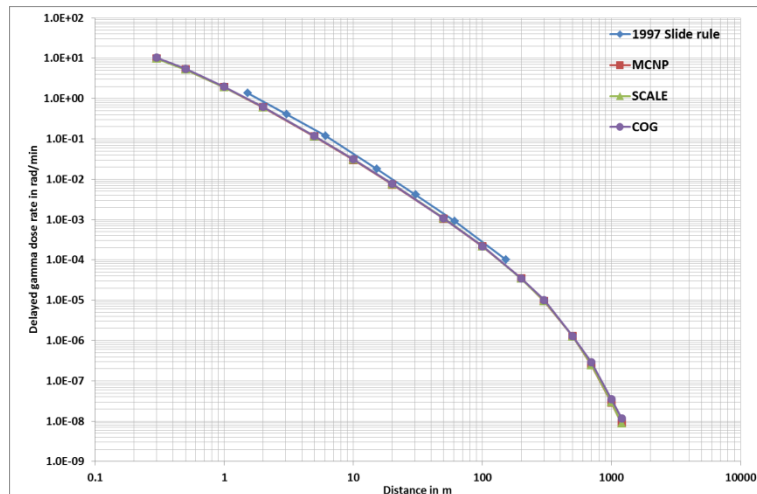


Figure 12. Comparison of delayed gamma dose rates for uranyl fluoride 10 min after the criticality accident

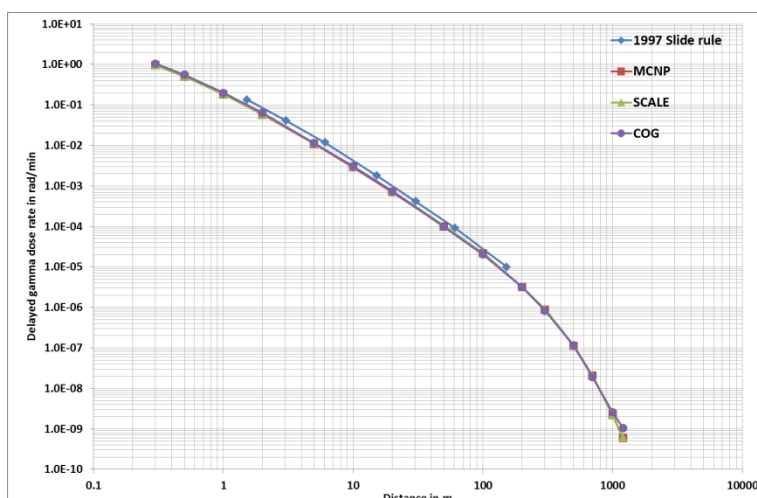


Figure 13. Comparison of delayed gamma dose rates for uranyl fluoride 100 min after the criticality accident

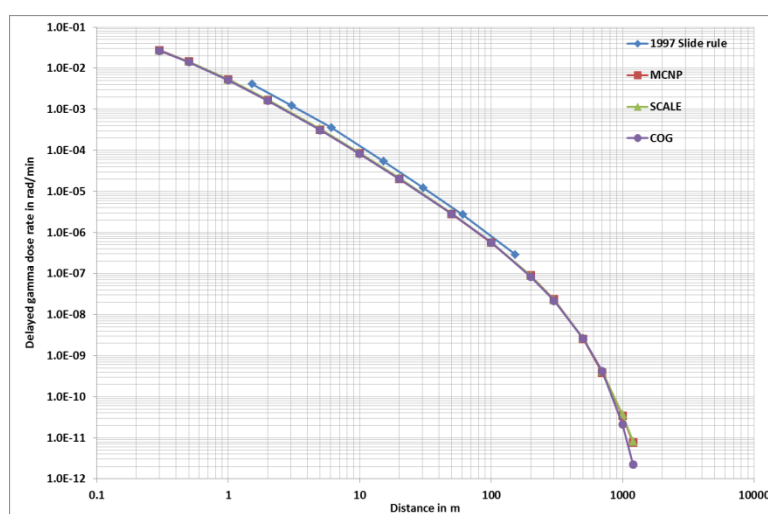


Figure 14. Comparison of delayed gamma dose rates for uranyl fluoride 1000 min after the criticality accident

The previous figures present the results for uranyl fluoride (case C1) but the following general observations are applicable for all the other cases (C2, C3, C4 and C5):

- the modern code results are higher than the 1997 Slide Rule for times less than 1 minute but as time increases (to 1 minute), this difference decreases,
- at 1 minute, the delayed modern code results agree very well with the 1997 Slide Rule,
- for times greater than 1 minute, the modern code results tend to be either slightly lower or equivalent to the 1997 Slide Rule, and this difference remains relatively constant and does not vary significantly with time. These general trends apply across all fissile media, though slight variations can occur depending on characteristics of these media (enrichment and moderation ratio which can have an impact on the delayed gamma source), as seen in Figure 15.

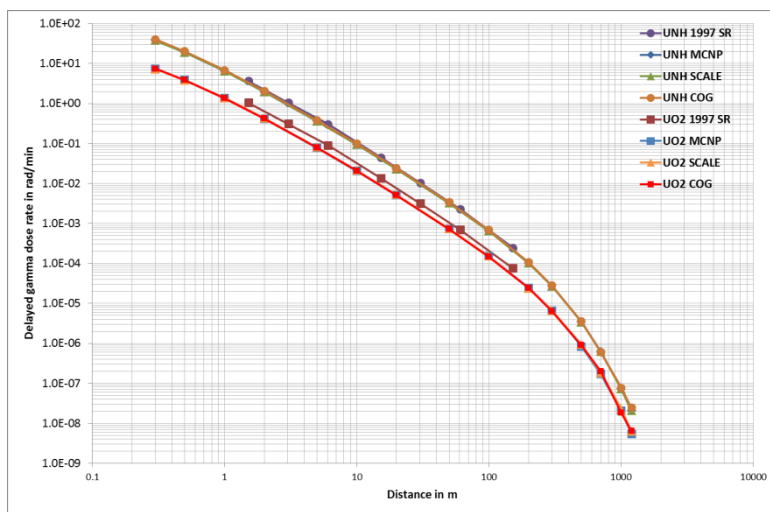


Figure 15. Delayed gamma dose rates for uranyl nitrate vs UO_2 , 10 min after the criticality accident

The complete explanation of these discrepancies is difficult to find because some assumptions made for the 1997 Slide Rule are unknown. However, the following elements can be suggested.

The first possibility to explain the discrepancies is the fact that ORIGEN data between 1997 and today has changed, with updated nuclear data. In particular for short decay times, the older gamma libraries were missing gamma spectral data for many of the short-lived fission products [16]. This might be the best explanation for the discrepancies observed for results for times less than 1 minute. Use of 1997 nuclear data to run ORIGEN today was not tested here but could be done in the future to confirm and quantify the nuclear data effect.

It can also be noticed that the modern code results are obtained by determining the instantaneous dose rate at a given time whereas the 1997 Slide Rule results considered an accumulated one-minute dose (integration of the dose rate over the next 60 s, which consider the intensity decrease of the source). So, a part of the discrepancies between modern codes and 1997 Slide Rule may be explained because the intensity of delayed gamma greatly decreases for short decay time (in particular lower than 1 minute). As an illustration, the intensity of delayed gamma (given in gamma per second) as a function of the decay time after the accident is presented in Figure 16 for the uranyl fluoride case and shows that between 1 second and 1 minute, the intensity decreases by a factor ~30. Thus, comparing instantaneous dose rate and integrated dose rate induces a bias for the shortest decay periods.

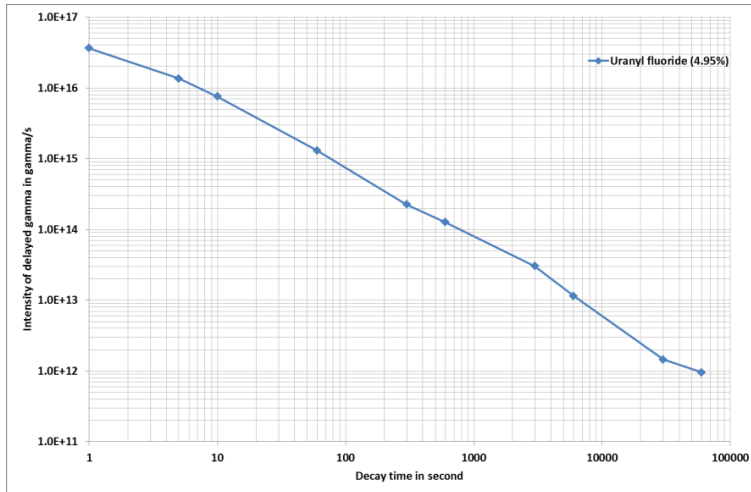


Figure 16. Intensity of delayed gamma as a function of the decay time for the uranyl fluoride

Finally, the 1997 Slide Rule states that “No delayed neutron contribution nor contributions from delayed gammas between 1 μ s and 1 s were included in the dose curves”. This assumption should have an impact on the results for the short times. The code-to-code comparison is illustrated in Figure 17 to Figure 21.

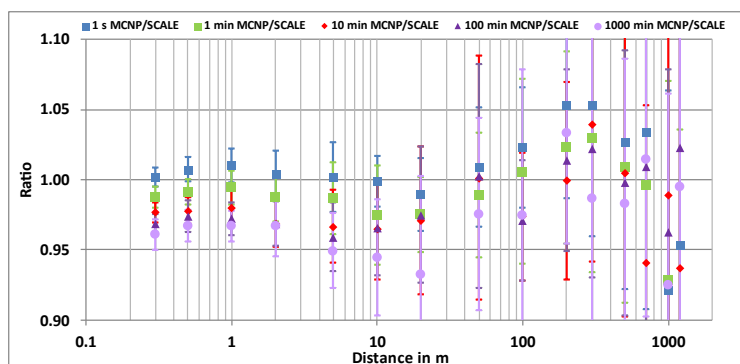


Figure 17. MCNP/SCALE delayed gamma dose rate ratio (with 2σ error bars) for enriched uranium metal

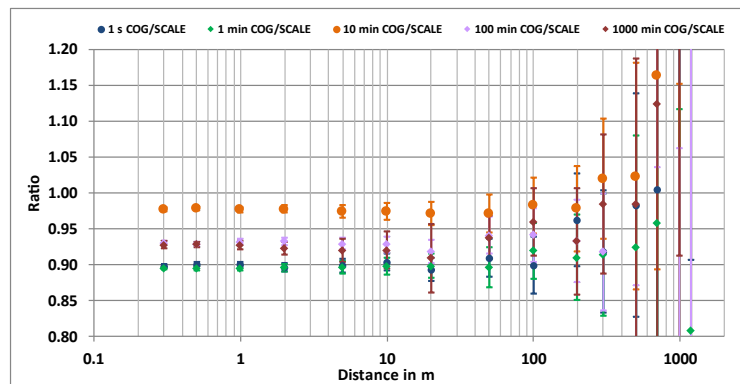


Figure 18. COG/SCALE delayed gamma dose rate ratio (with 2σ error bars) for enriched uranium metal

It can be seen that the discrepancies between codes increase with the distance after 500 meters. It may be explained by important uncertainties in the doses calculation results and not necessarily by a difference in the delayed gamma source. At 10 meters from the criticality accident (with no convergence issues and a relative error on the ratio less than 2 %), the Figure 21 shows the comparison for all cases. Two behaviors can be observed. The comparison between MCNP and SCALE results shows a slight decrease trend with decay time. A possible explanation is that the delayed gamma sources were determined with the same “method” but with different options (in particular the energy binning) and code versions, which have an impact in particular on the source’s intensity

for long decay time. The comparison between COG and SCALE shows an "up and down" behavior. The COG/SCALE delayed gamma dose rate ratio present a slightly important discrepancy (0.81 – 0.94) for short time (less than 1 min), then a swing behavior (1 - 1.14) to finally come back to lower values (0.87 - 1). This behavior needs to be investigated.

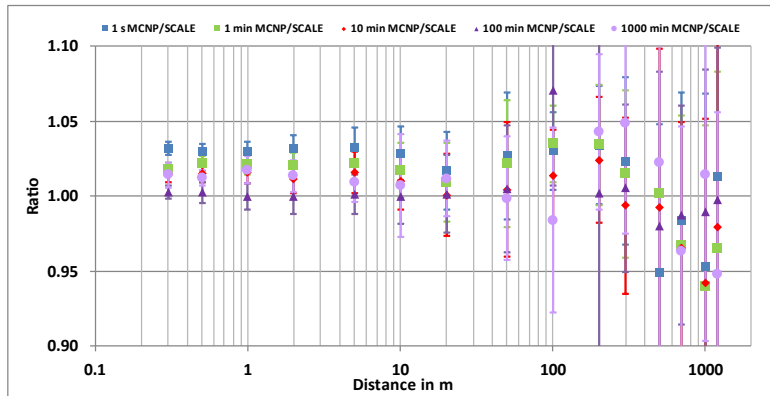


Figure 19. MCNP/SCALE delayed gamma dose rate ratio (with 2σ error bars) for uranyl fluoride

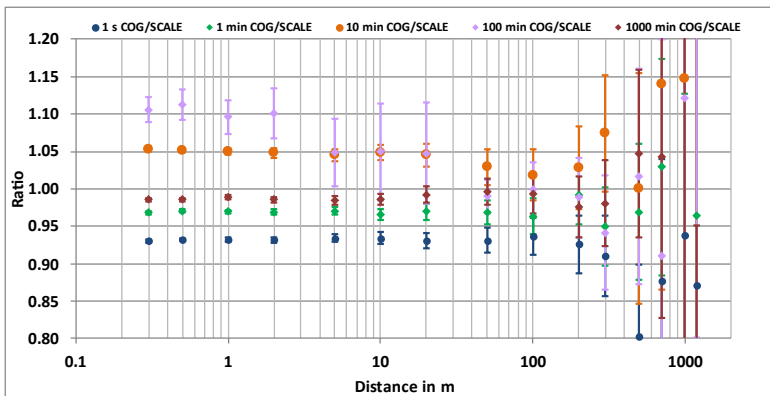


Figure 20. COG/SCALE delayed gamma dose rate ratio (with 2σ error bars) for uranyl fluoride

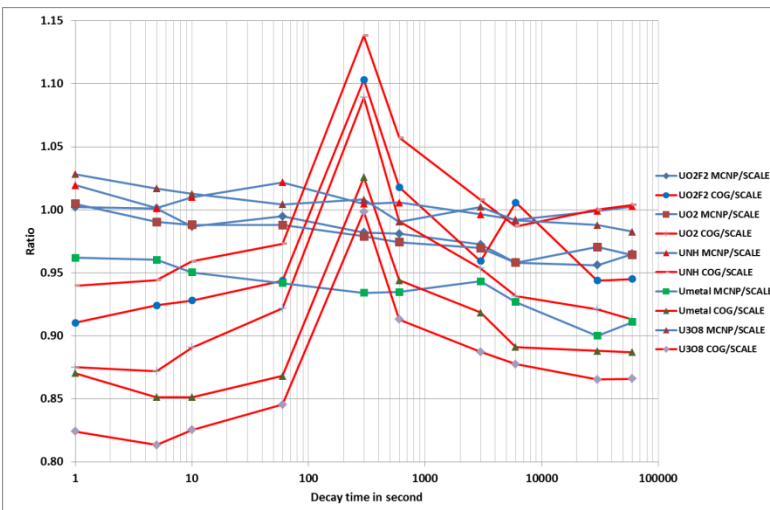


Figure 21. Code-to code delayed gamma dose rate ratio for all cases at 10 meters from the criticality accident.

Regarding the determination of the delayed gamma source, some discrepancies occurred between codes. The detailed analysis of these discrepancies was not the main purpose of this report, but additional effort should be done in order to understand the discrepancies.

4.3. Sensitivity studies

This section outlines a series of sensitivity studies conducted on unshielded configurations to evaluate how changes in humidity, ground composition, and the configuration of the surrounding air volume (commonly referred to as the 'skyshine' effect) affect radiation dose calculations. Calculations were performed for a thermal system (Case 1 – U(4.95)O₂F₂ – H/²³⁵U = 410) and a fast system (Case 4 – U(93.2wt%) metal – H/²³⁵U = 0). The complete results from these calculations are compiled in Appendix 3. All plotted ratios include 2σ ($\sigma \leq 10\%$) error bars. Data series are labeled as follows: N for neutrons, P for photons, and C1/C4 for thermal/fast systems (Case 1 and Case 4). All groups involved used the ANSI/HPS 13.3-2013 response function. The term "Original MCNP" refers to the calculations performed under reference conditions without shielding, serving as the baseline for these sensitivity studies, referred to as "Perturbed MCNP." MCNP 6.1 was used consistently for all sensitivity studies. Although other laboratories performed similar studies with their respective codes, only results obtained with MCNP are presented here, as the outcomes from other codes were found to be equivalent.

4.3.1. Air composition

Dry air was considered for the initial calculations. In order to determine the impact of water (moisture) in the air, the prompt neutron and gamma doses are calculated considering 10% and 100% humidity. The air composition used is given in the task specification [17]. Dry air compositions are different from those used for the calculations of historical Slide Rules [1]-[2].

Figure 22 presents the ratios of prompt neutron and gamma doses calculated with a relative humidity "RH" of 10% and 100% (0.016 and 0.163 wt.% H) to the one calculated with dry air as a function of detector location.

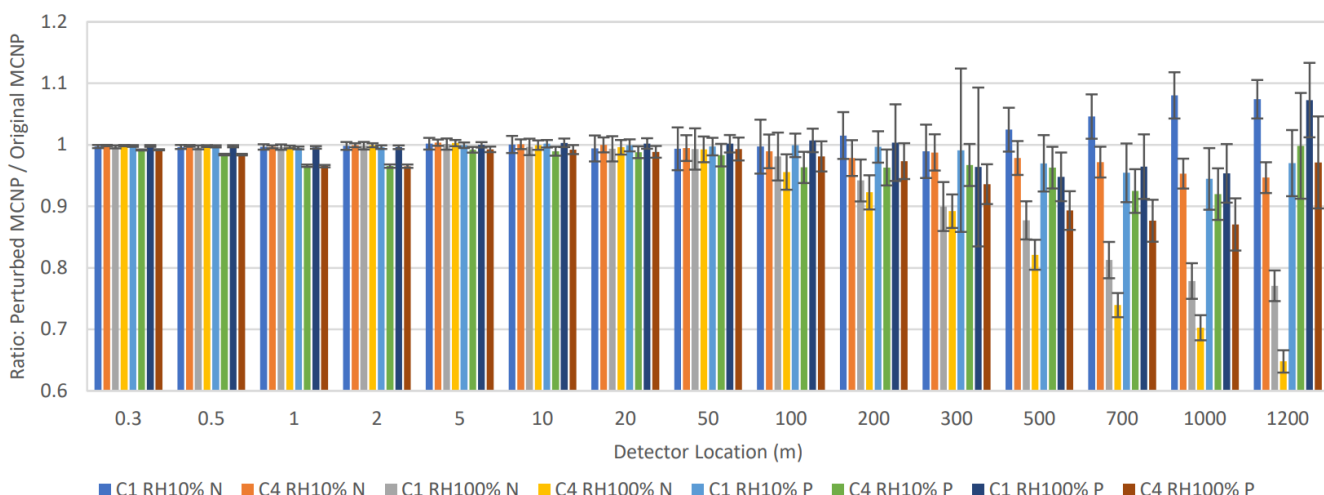


Figure 22. Ratio of prompt doses calculated with air humidity to the prompt doses calculated with dry air.

The results presented in the figure above highlight the moderating effect of water on the prompt neutron and gamma doses. This effect is more pronounced for the prompt neutron dose, which is reduced by nearly 35% for a humidity of 100% compared to dry air. The effect of humidity is less significant for the prompt gamma doses, as the calculated doses are reduced by nearly 10% for the most distant detectors. For the different configurations studied, the air humidity has no significant effect for measurement distances less than 100 m.

4.3.2. Ground composition and dimensions

This section evaluates the effects of changing the ground composition used in the first phase from regulatory concrete (containing 1.0 wt% H) to dry soil – referred to as “earth” – on the original Slide Rule. Moreover, the ground dimension was changed from 30.48 cm (initial configurations) to 50 cm.⁷

⁷ An increase in the thickness of the concrete ground (from 30.48 cm to 50 cm) has no significant effect on the neutron and photon dose.

Figure 23 presents the ratios of the prompt neutron and gamma doses calculated with a 50 cm thick soil of “earth” composition, to the doses calculated with a 50 cm thick concrete ground. The ground and concrete material compositions used are given in the task specification [17].

The choice of these materials for the floor is explained by the fact that the “concrete” medium is hydrogenated while the “earth” medium is non-hydrogenated. Moreover, these two media adequately represent the main media present in the vicinity of a nuclear installation.

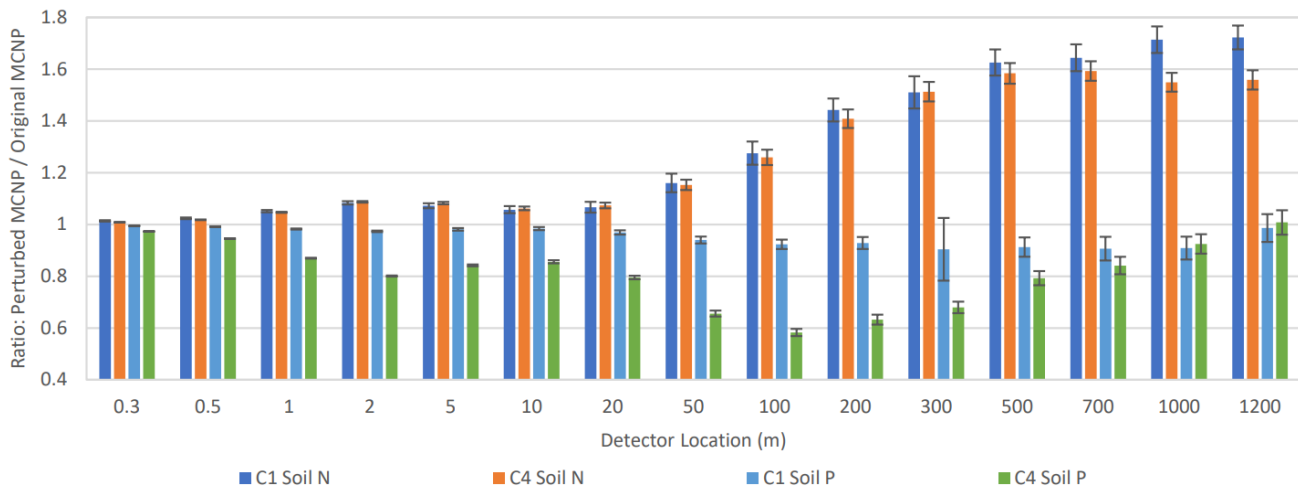


Figure 23. Ratio of prompt doses for 50 cm dry soil to those for 30.48 cm ‘concrete’ soil.

Changing the ground composition has a relatively minor impact on the photon dose for the uranyl fluoride sphere (case 1 or C1). For the uranium metal sphere (case 4 or C4), the presence of dry soil initially leads to a reduction of photon dose, up to 40%, before increasing to a value similar to the original simulation. Considering dry soil leads to an increase of the neutron dose for both cases (C1 and C4), by more than 40% for the longest distances (over 300 m).

4.3.3. Skyshine

The skyshine effect is the contribution to the total dose of the volume of air located at an altitude greater than 10 m. To determine the skyshine effect, calculations are made by reducing the height of the external air volume (sky height) from 1 500 m to 10 m.

Figure 24 shows the ratios between prompt doses calculated with a sky height of 10 m to those calculated with a sky height of 1500 m. The ground thickness is 30.48 cm for these calculations. Ratios are calculated for cases 1 and 4.

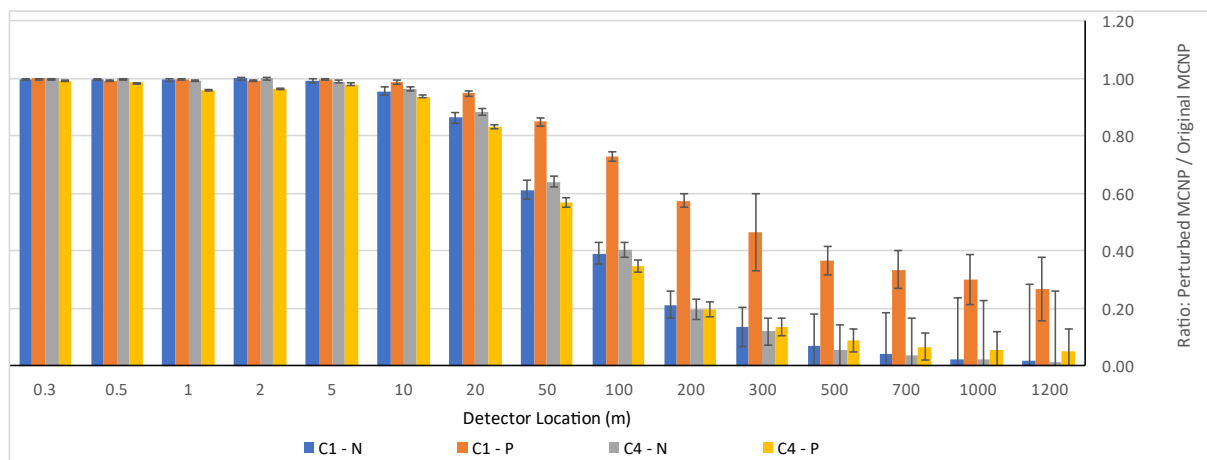


Figure 24. Ratio of prompt doses for a 10 m sky height to those for a 1.5 km sky height.

The results show that the sky effect has a significant contribution (over 10%) to prompt doses measured at distances greater than 20 m.

4.4. Shielded configurations

This paragraph details the computations carried out about the impact of radiological screens nature on prompt doses for case 1 ($\text{U}(4.95\text{wt\%})\text{O}_2\text{F}_2$) and case 4 ($\text{U}(93.2\text{wt\%})$ metal). The positions of the detectors, screen compositions, and thicknesses used are described in the phase 3 task specifications [17].

Four different shielding materials (stainless steel 304, water, lead, and concrete) are modeled at halfway between the source and the detector⁸. The dimensions of the screen are “infinite” in the Y and Z directions (with the X direction corresponding to the thickness of the screen).

For the stainless steel 304, water, and lead, the following thickness are considered: 1, 5, 10 and 20 cm. The regulatory concrete was simulated with thicknesses of 20 and 40 cm.

The dose ratio between configurations with and without shielding materials are presented in Figure 25 – Figure 32 with the complete corresponding values compiled in Appendix 4. All cases treated by ASNR were performed using MCNP 6.1. In some specific cases where MCNP results were not available due to incomplete simulations, SCALE results are presented instead. While SCALE results are consistent with MCNP and COG, they provide an alternative baseline for comparison under similar conditions (see §4.4.5).

Each laboratory involved used the same flux-to-dose conversion factors published in the ANSI/HPS 13.3-2013 standard on criticality accident dosimetry [20]. All the Monte Carlo results and ratios plotted include 2σ ($\sigma \leq 10\%$) error bars, and all data series in the plots are labeled N for neutron and P for photon.

4.4.1. Water

For both cases, the neutron doses decrease because of the thickness of water shielding. The decrease is slightly dependent on the distance from the source. The largest neutron dose reduction was about 96% for a water thickness of 20 cm.

Regarding the gamma dose, the conclusion depends on the case. For case 1 (UO_2F_2), the dose decreases with the water thickness, up to 50% at 20 cm. However, for the case 4 (uranium metal) presented in Figure 26, the photon dose initially increased almost by a factor of 2 due to the production of photons in the water shield. This increase is maximum when the distance between the source and the water is small. At large distances, the photon dose reduction is similar to the one observed for case 1. For the water shield, the photon dose tended to be as large or larger than the neutron dose.

⁸ The distance edge-to-edge between the source and the screen is half the edge-to-edge distance between the source and the detector.

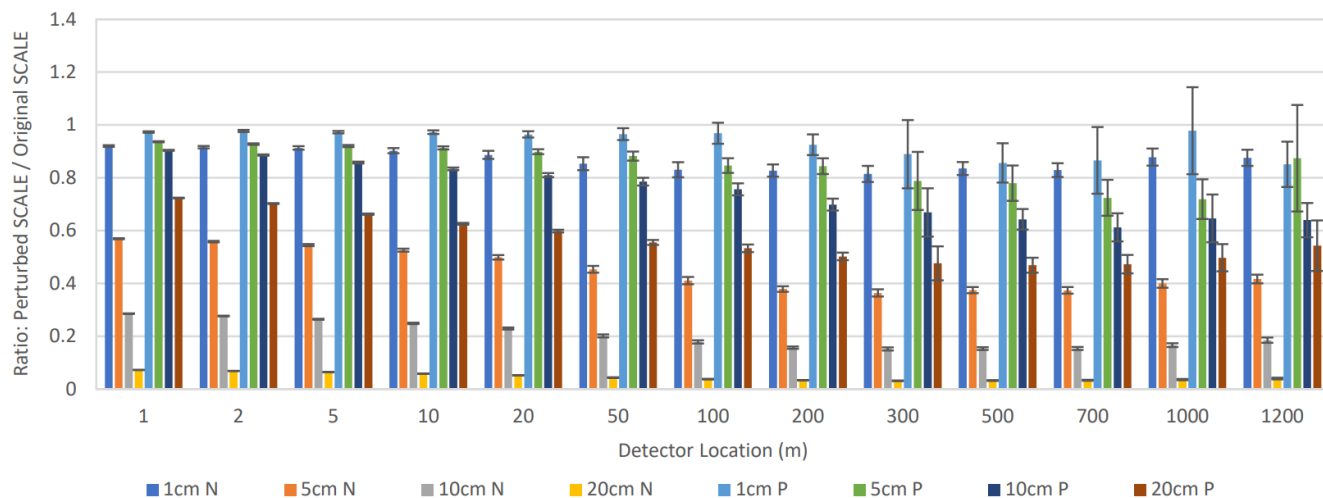


Figure 25. Case 1 – Water – Ratio of prompt doses with shield to without shield.

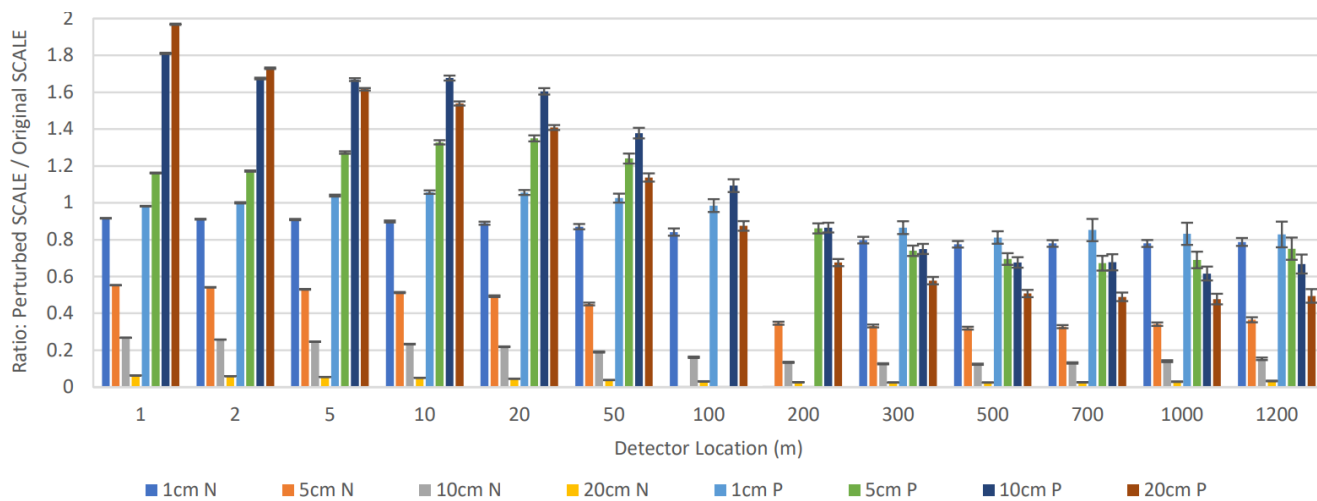
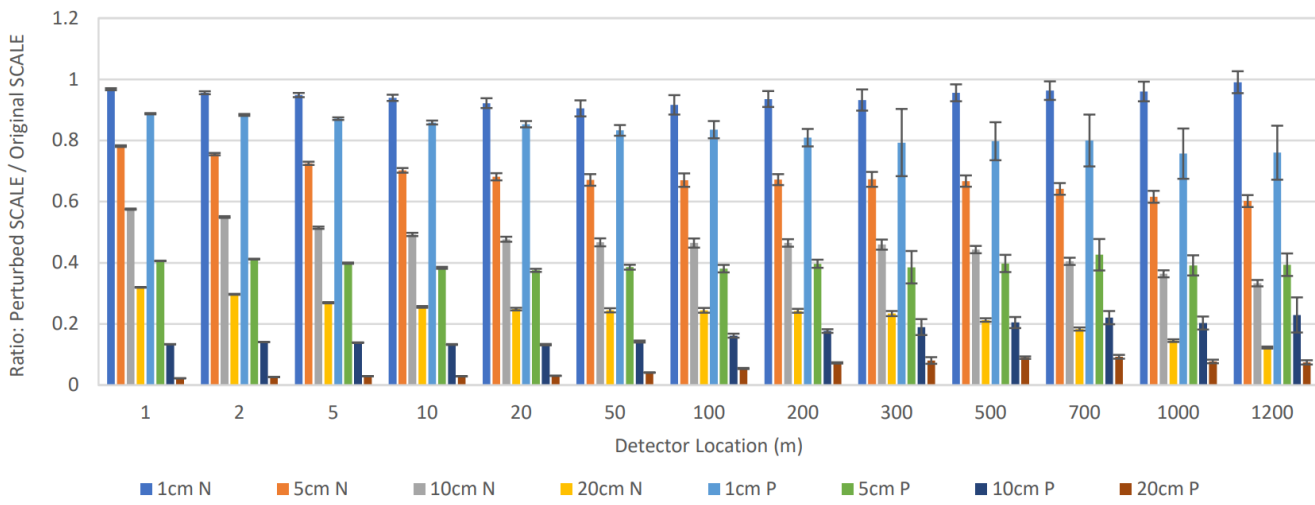
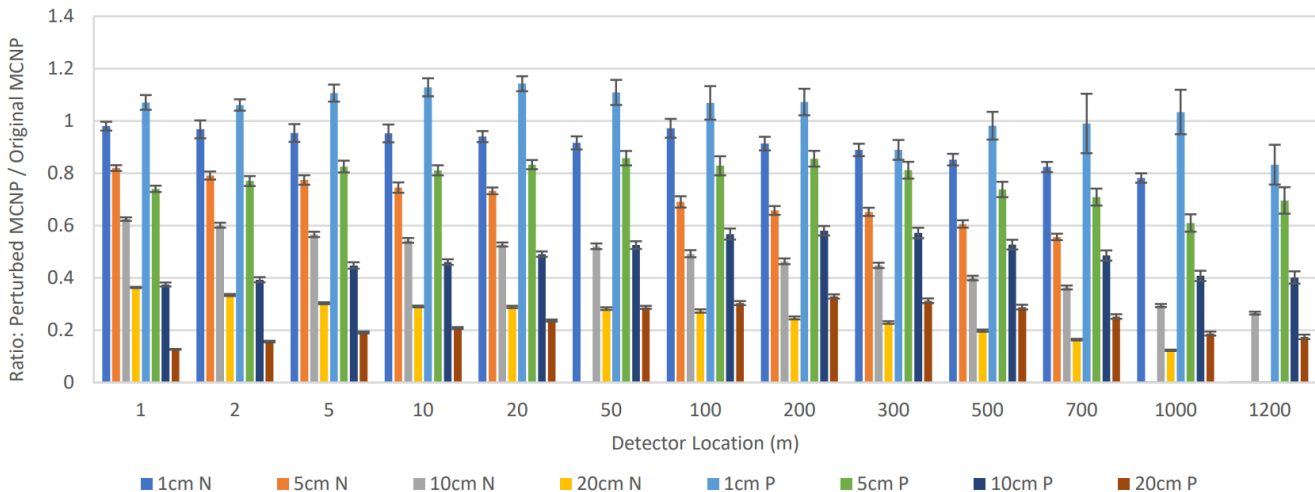


Figure 26. Case 4 – Water – Ratio of prompt doses with shield to without shield.

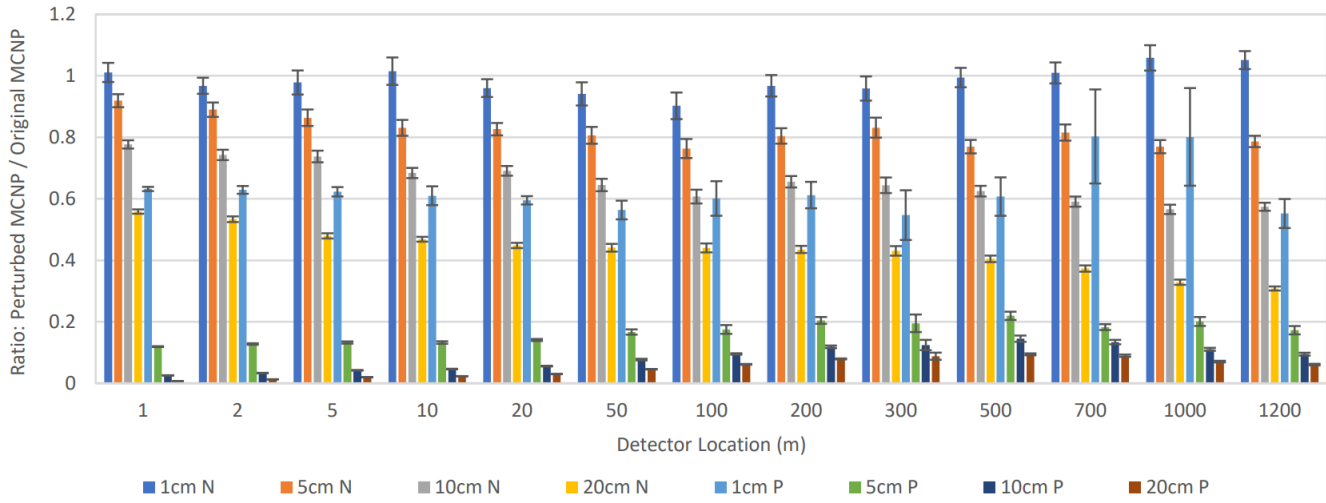
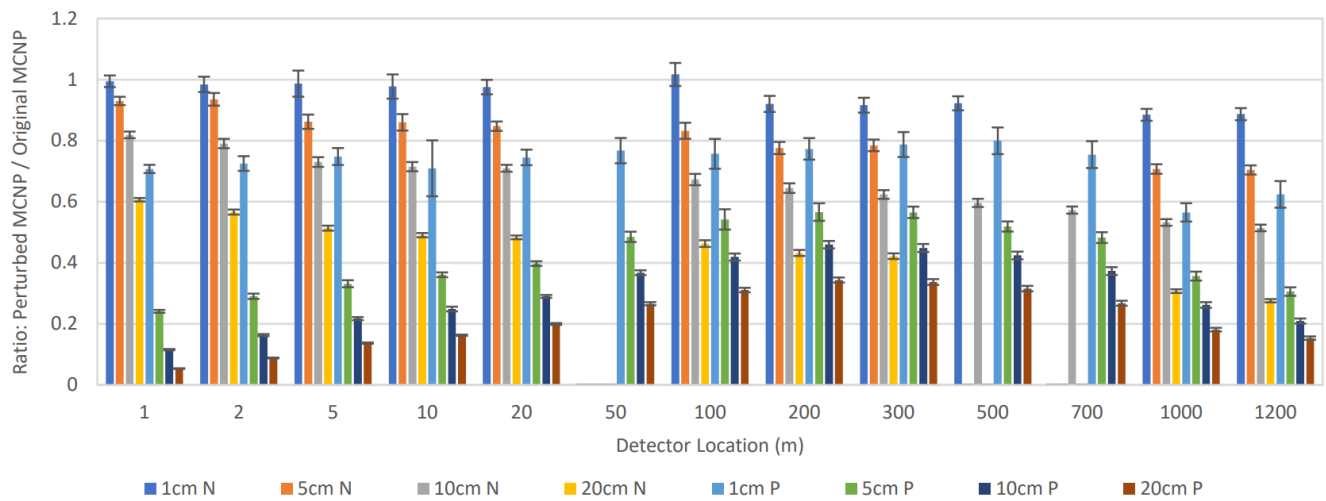
4.4.2. Steel

For the uranyl fluoride source (Figure 27), the impact of the stainless steel 304 shield is close to the one observed for water shielding. However, the neutron dose tended to be larger than the photon dose with the stainless-steel shield. The largest decreases for the neutron and photon doses were 87% and 97%, respectively. The neutron dose was decreased for the uranium metal sphere (Figure 28) with the stainless-steel shield, and the photon dose increased slightly (at most 14%) out to about 200 m, and then it decreased. The largest decrease for both the neutron and photon doses was about 87%.

**Figure 27. Case 1 – SS304 – Ratio of prompt doses with shield to without shield.****Figure 28. Case 4 – SS304 – Ratio of prompt doses with shield to without shield.**

4.4.3. Lead

The effect of the lead shields on neutron and photon doses is similar for the uranyl fluoride (Figure 29) and uranium metal (Figure 30) sources. The neutron and photon doses always decreased with the lead shield thickness, and the neutron doses is always larger than the photon doses. For the uranyl fluoride sphere, the largest decrease for the neutron and photon doses was 69% and 98%, respectively. For the uranium metal sphere, the decreases were 72% and 86%.

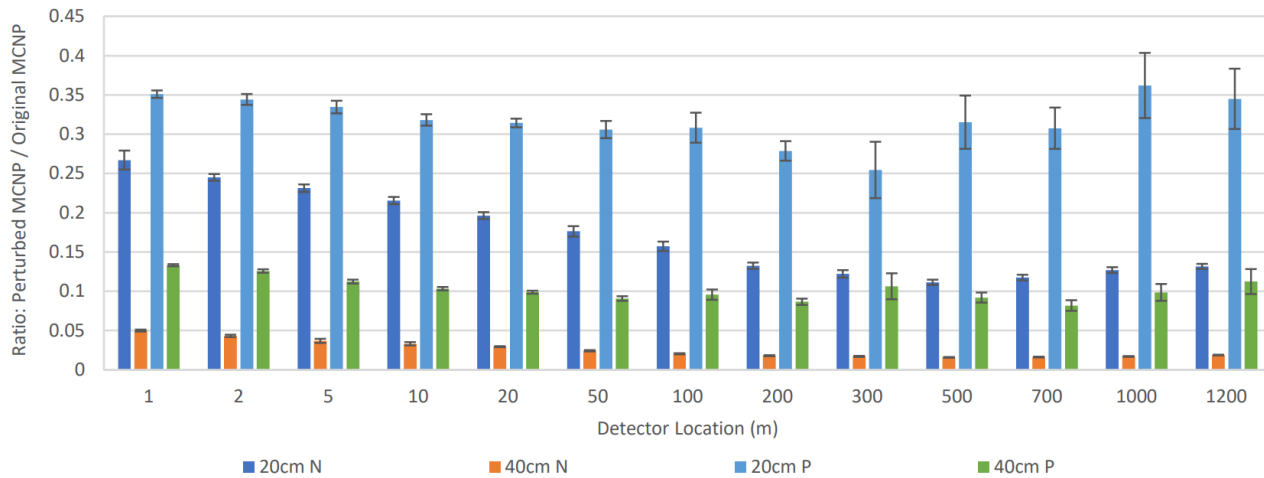
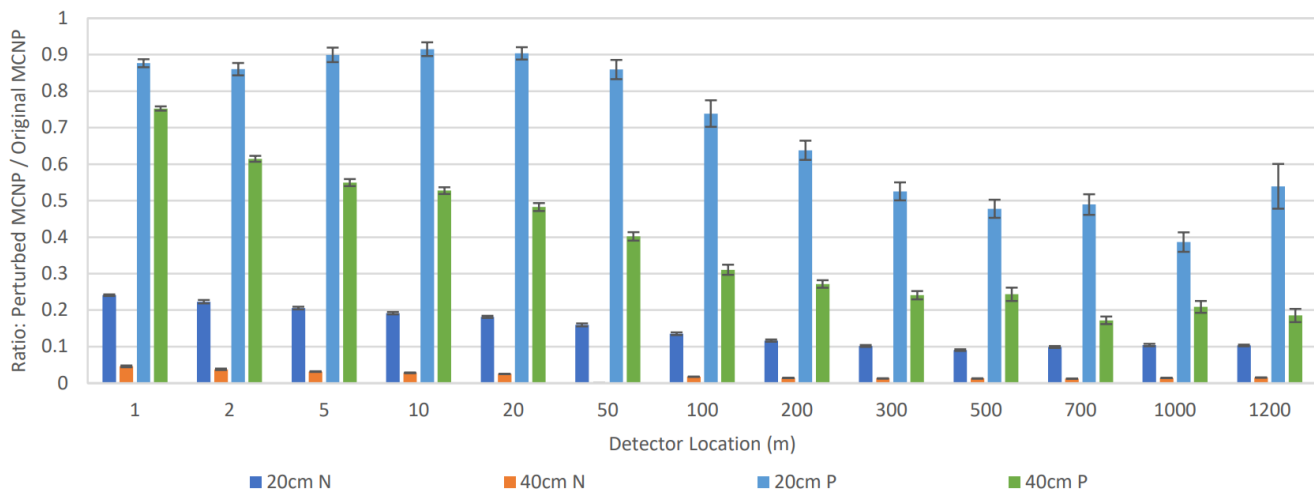
**Figure 29. Case 1 – Lead – Ratio of prompt doses with shield to without shield.****Figure 30. Case 4 – Lead – Ratio of prompt doses with shield to without shield.**

4.4.4. Concrete

For both cases, the concrete shield decreased the dose. For neutron dose, the diminution increases with the distance to detector and shield thickness. For photon dose, the dose diminution is largely higher for case 1 compared to case 4.

For case 1 (Figure 31), the neutron dose decrease stops for a distance higher than 200 m. At this point, the photon dose increased slightly. In all instances, the photon dose was larger than the neutron dose. The largest decreases for the neutron and photon doses were 98% and 91%, respectively.

For case 2 (Figure 32), the neutron and photon decrease stops for distance higher than 300 m. The largest decreases for the neutron and photon doses were 98% and 82%, respectively.

**Figure 31. Case 1 – Concrete – Ratio of prompt doses with shield to without shield.****Figure 32. Case 4 – Concrete – Ratio of prompt doses with shield to without shield.**

4.4.5. Code-to-code comparison

A comparison between MCNP, SCALE, and COG results is presented below for configuration involving concrete shielding. Figure 33 and Figure 34 present the prompt dose ratio between SCALE and MCNP for cases 1 and 4. Figure 35 and Figure 36 present the prompt dose ratio between COG and MCNP for cases 1 and 4.

The results for all codes are statistically equivalent, or they differ by less than 10%. COG results for high distance (500 m and beyond) have uncertainties greater than 10% and would benefit from additional run time to improve the Monte Carlo statistics.

The results presented in this section for concrete are representative of all the results obtained for other shielding. The agreement between MCNP, SCALE, and COG is fairly good, with only small, statistically significant differences observed.

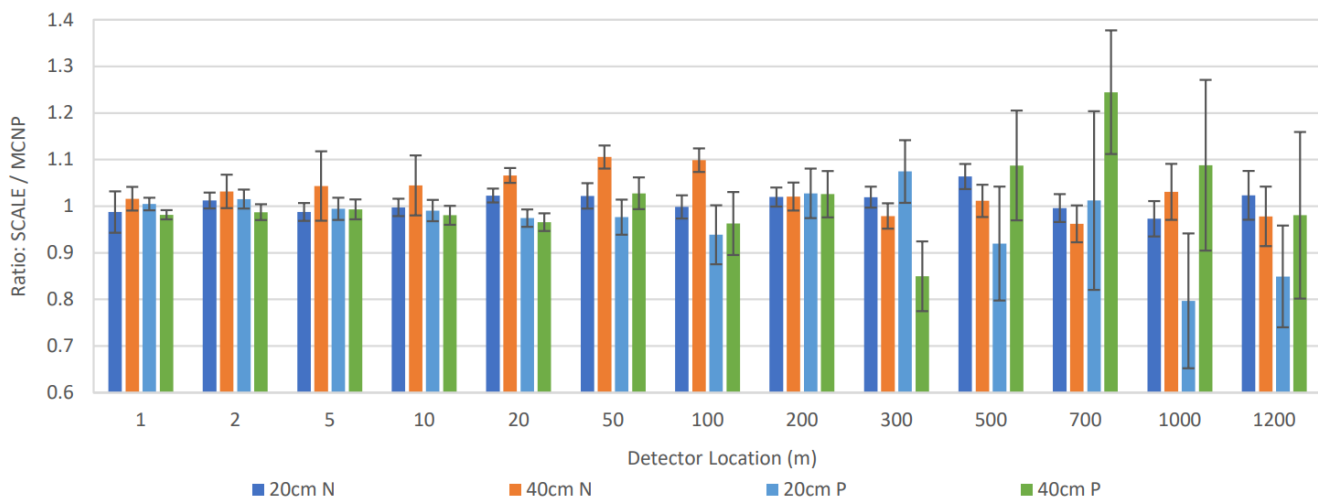


Figure 33. Case 1 – Concrete – SCALE-to-MCNP doses ratio.

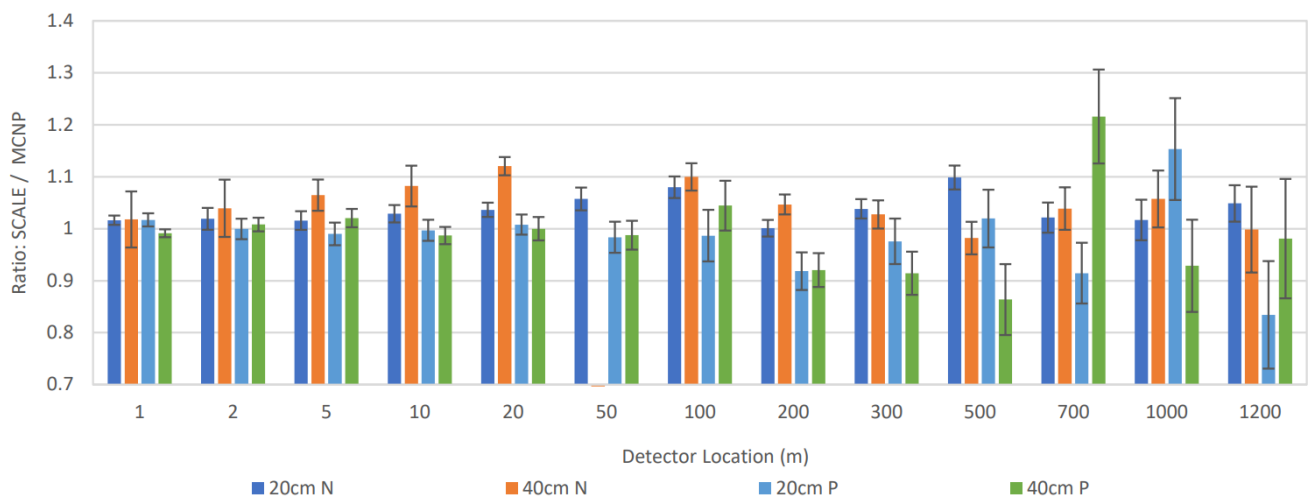


Figure 34. Case 4 – Concrete – SCALE-to-MCNP doses ratio.

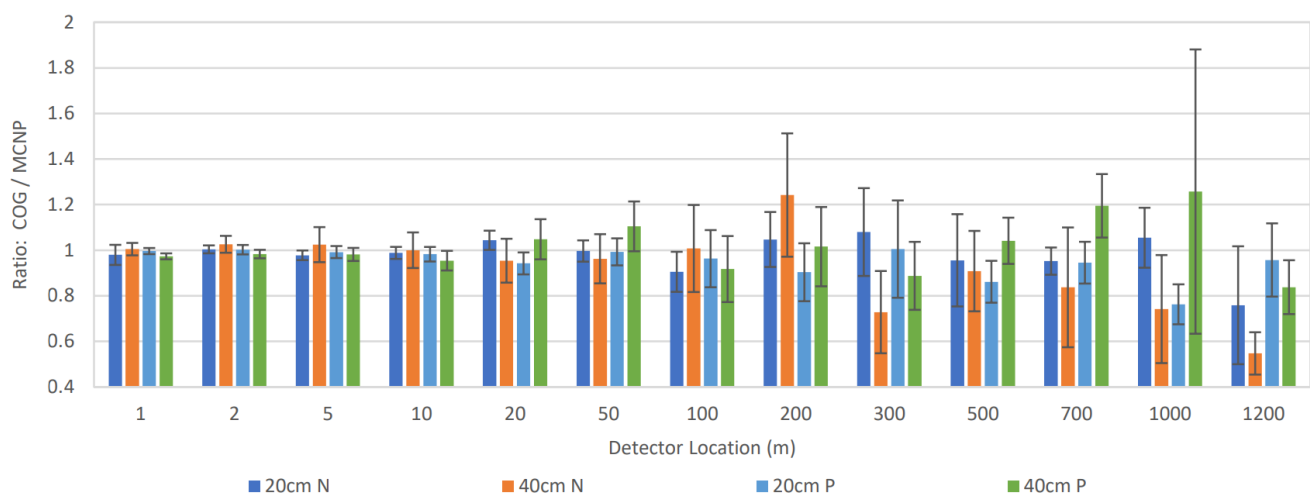
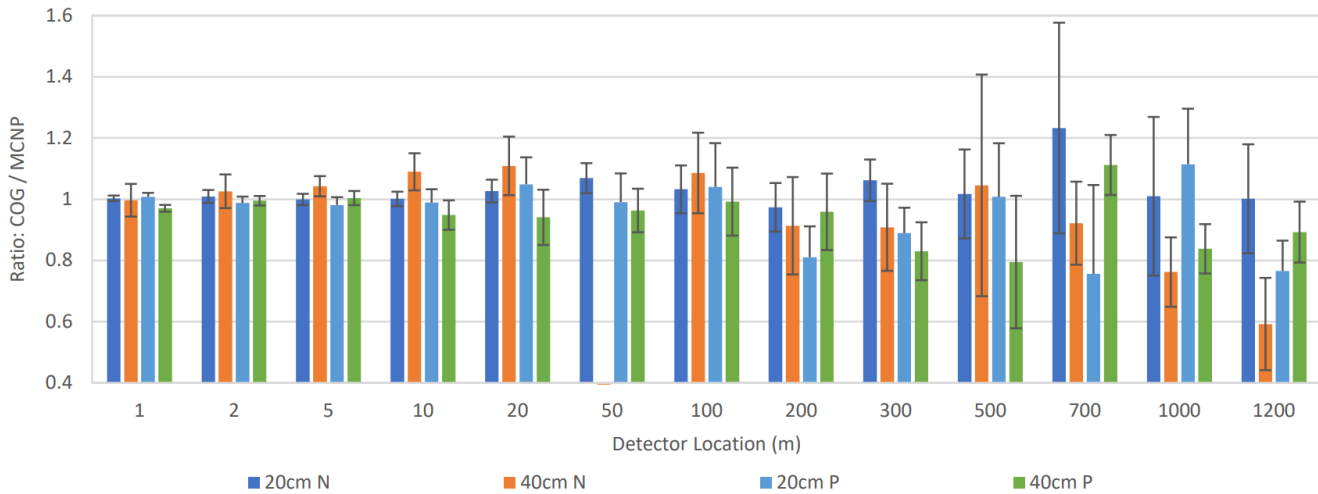
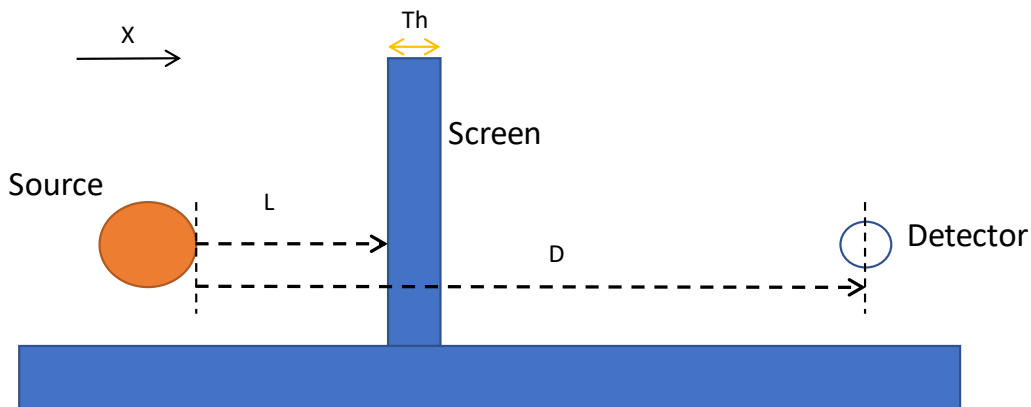


Figure 35. Case 1 – Concrete – COG-to-MCNP doses ratio.

**Figure 36. Case 4 – Concrete – COG-to-MCNP doses ratio.**

4.4.6. Impact of screen position

Besides its composition and thickness, this section discusses the impact of the screen's position on the effectiveness of shielding materials in radiation protection.



For the computations presented in the previous sections, the distance labeled "L" is always half distance of "D", which refers to the distance between the source edge and the center of the detector.

This section explores the impact of the shielding material's distance to the source by considering six positions, corresponding respectively to 1/4, 1/3, 1/2, 2/3, 3/4, and 4/5 of distance "D". These positions are numbered from 1 to 6 for ease of reference.

Given the vast number of potential configurations (over 10,000 possible configurations for one case), only prompt neutron doses are analyzed for case 4 at six detector distances: 1 m, 2 m, 5 m, 10 m, 50 m, and 100 m. The study uses a consistent shield thickness (20 cm) and composition (concrete), and the results, displayed in Figure 37 represent the prompt neutron dose ratios with and without the screen for each position⁹.

The combined Monte-Carlo (σ) uncertainties are less than 3%.

⁹ Data points beyond position 3 for d_1m are not shown due to unavailable results. Additional simulations are being considered to address this gap.

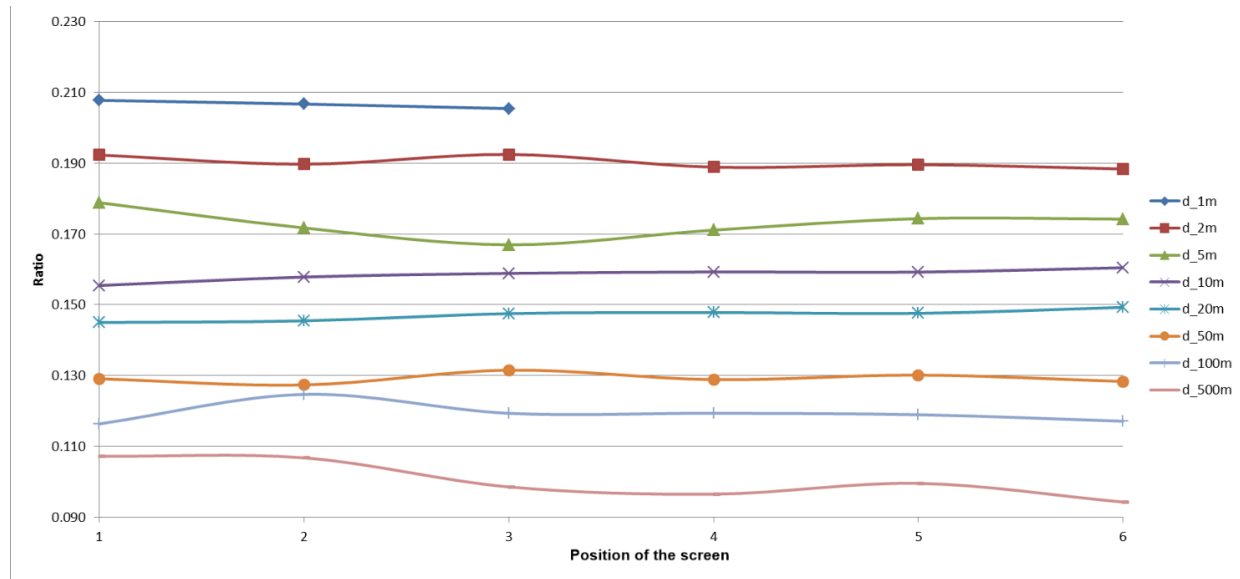


Figure 37. Case 4 – N – Concrete (20 cm) – Ratio of neutron prompt doses with and without screen for six screen positions.

Analysis of these configurations does not allow us to define a general behavior for all screens. Nevertheless, it seems that the position of the screen in relation to the source has little or no influence on the effect of the calculated dose.

Future studies could investigate whether the screen's position similarly affects gamma doses, to confirm or refute the absence of impact observed with neutron doses.

5. PLUTONIUM CONFIGURATIONS

This chapter discusses the results for new configurations (phase 2) dealing with plutonium systems, calculated by modern 3D radiation transport codes, i.e. MCNP, SCALE and COG.

5.1. Model description

The geometry for phase 2 is derived from the 1997 Slide Rule model. It consists of a simple 2-D air-over-ground configuration with the source located at the radial center of a right-circular cylinder. The radius and the height of the air cylinder is 1530 m. The centers of the critical assemblies (spheres or cylinders) are all 1 m above the ground. The ground is now modelled as a 50 cm layer of the same concrete (the initial configuration and the phase 1 configuration considered 1 ft or 30.48 cm of concrete). Additional calculations on uranium system, see §4.3.2, demonstrated that this modification has no impact on dose results for a ground made of concrete.

Figure 2 and Figure 3 present the model for these initial calculations. For more clarity, all the information needed to calculate the phase 2 configurations were written in specific documents using a “benchmark format” [19].

Neutron and gamma doses were calculated as a function of distance from 0.3 m to 1200 m. The distance between the source and the detector is measured from the external surface of the source (either plutonium for bare geometry or steel when the reflector is considered) to the center of the detector. The detector used for phase 2 was chosen to be a cylindrical shell with a square cross-section of 5 cm x 5 cm to take advantage of the symmetry of the problem. The center of the detector is also at a height of 1 m above the ground.

The calculations include five moderation ratios for plutonium spheres ($H/Pu = 0, 10, 100, 900, 2000$). These moderation ratios represent different compositions of plutonium moderation, ranging from pure plutonium metal (without moderator) to highly moderated configurations.

5.2. Results

This section presents and discusses the simulation results for the plutonium cases. As specified in reference [19], 690 results¹⁰ are needed to cover all the cases for phase 2. The laboratories used various codes and methods, presented in chapter 3. Each participant has used the flux-to-dose conversion factors provided in the ANSI/HPS N13.3 standard [20] to compare their results. This standard is specifically dedicated to the dosimetry of a criticality accident and deals with deterministic consequences of a criticality accident. Other conversion factors could be used in the future to compare the results obtained. In addition, some participants have performed plutonium calculations with the Henderson flux-to-dose conversion factors to compare not only the dose given by uranium systems (phase 1) and plutonium systems (phase 2) but also the two flux-to-dose conversion factors (ANSI/HPS N13.3 and Henderson) applied to plutonium systems. Based on results from phase 1, good agreement was observed between participants and with the original Slide Rule on prompt doses (neutron and gamma). On the contrary, some discrepancies were found between participants and with the original de Rule on delayed gamma doses, see § 5.3.

5.2.1. Bare sphere calculations

The complete dose results for plutonium are presented in Appendix 2. Figure 38 and Figure 39 show the neutron and gamma prompt dose for the bare spherical plutonium systems calculated with MCNP with the ANSI/HPS N13.3 flux-to-dose conversion factors. For a given distance, the neutron dose is higher when the moderation ratio (H/Pu) is lower. The difference between the extreme cases goes from a factor of 13 for short distances to a factor of 4.5 for long distances. Regarding prompt gamma doses, the lowest dose is obtained for the metal plutonium system whereas the highest dose is obtained for an intermediate moderation ratio. At short distances, the difference between the extreme cases is a factor of 5 on prompt gamma doses. After 500 meters,

¹⁰ for bare sphere configurations: 5 cases (moderation ratios) x 15 distances x 2 particles (N or P)

+ for cylinder plutonium configuration: 2 cases x 15 distances x 2 particles (N or P) x 3 types of vertical cylinder

+ for reflected configurations: 2 cases x 15 distances x 2 particles (N or P) x 6 reflector thicknesses

all the gamma curves become closer with a maximum ratio of 1.5. All these observations can be roughly explained by the various self-absorption inside the sphere and by the fact that neutrons are produced only in the plutonium sphere whereas prompt gammas are produced not only in the plutonium sphere but also by neutron with (n, gamma) reactions within the surrounding environment (mainly from the ground in these configurations).

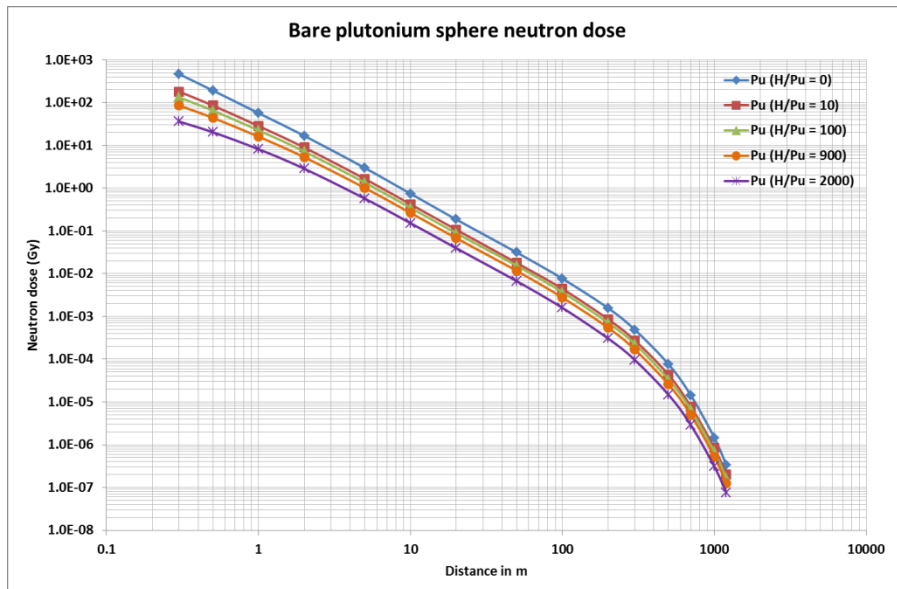


Figure 38. Neutron prompt doses for bare plutonium sphere calculated with MCNP

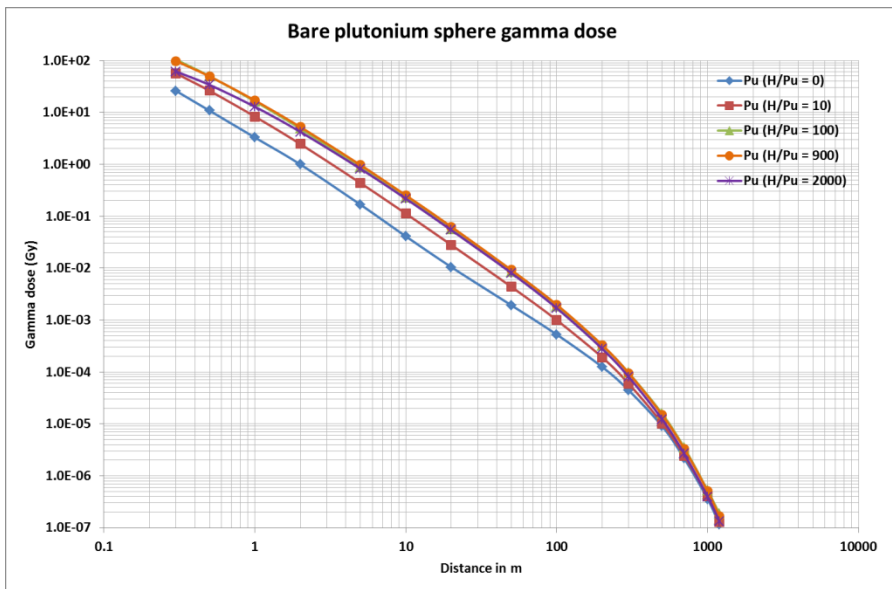


Figure 39. Gamma prompt doses for bare plutonium sphere calculated with MCNP

Figure 40 shows the neutron/gamma prompt dose ratio for the bare spherical plutonium system. For all the moderation ratios, the neutron/gamma dose ratio is relatively constant from 0.3 meter up to 20 meters. Beyond 20 meters, the ratio constantly decreases for metal plutonium whereas it continues to increase then decreases after 500 meters for other configurations.

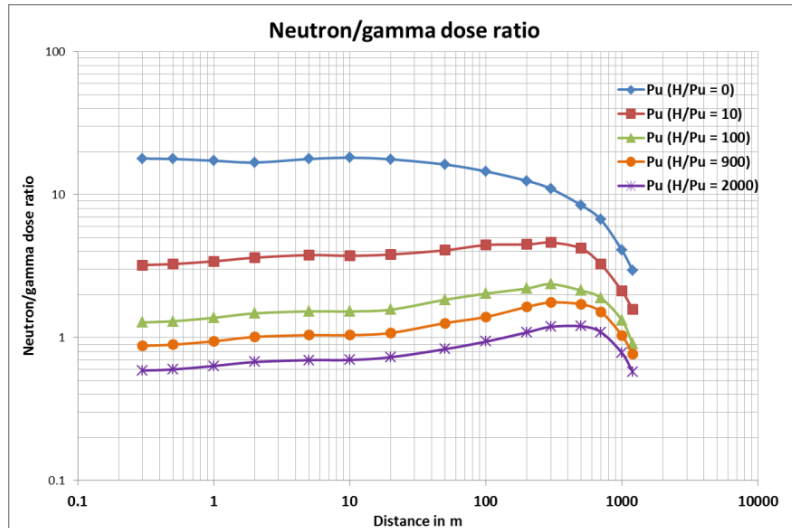


Figure 40. Neutron/gamma prompt dose ratio for bare plutonium sphere calculated with MCNP

Figure 41 presents the code-to-code comparison of neutron and gamma prompt doses for the bare plutonium sphere. Good agreement is observed between codes with discrepancies generally lower than 5 %. At long distances, the discrepancies between codes are higher (without any trend) but with higher uncertainties. Generally, the relative error (2σ) on the code results is lower than 2 % until 500 meters and up to 10 % at long distances. For prompt gamma doses, a small discrepancy between codes is perceptible and might be due to the different treatment of bremsstrahlung by these codes. MCNP's thick target bremsstrahlung model accounts for the electromagnetic cascade of gammas and electrons that produce many low energy bremsstrahlung gammas and allows users to not perform electron transport for geometries with thick shielding materials. All of SCALE's fixed-source radiation transport codes use gamma production data based on ENDF, which does not include this sort of bremsstrahlung. When this model is turned off (PHYS:P j 1), the MCNP and SCALE results are statistically the same. Regarding COG, whenever an electron-producing photon reaction occurs, COG checks whether the reaction occurred in a region enabled by the user for electron transport. If not, which is the case here, then the electron energy is immediately deposited. All these observations regarding code-to-code comparison could be applied to the other kind of calculations performed in this chapter (no bremsstrahlung photons are transported).

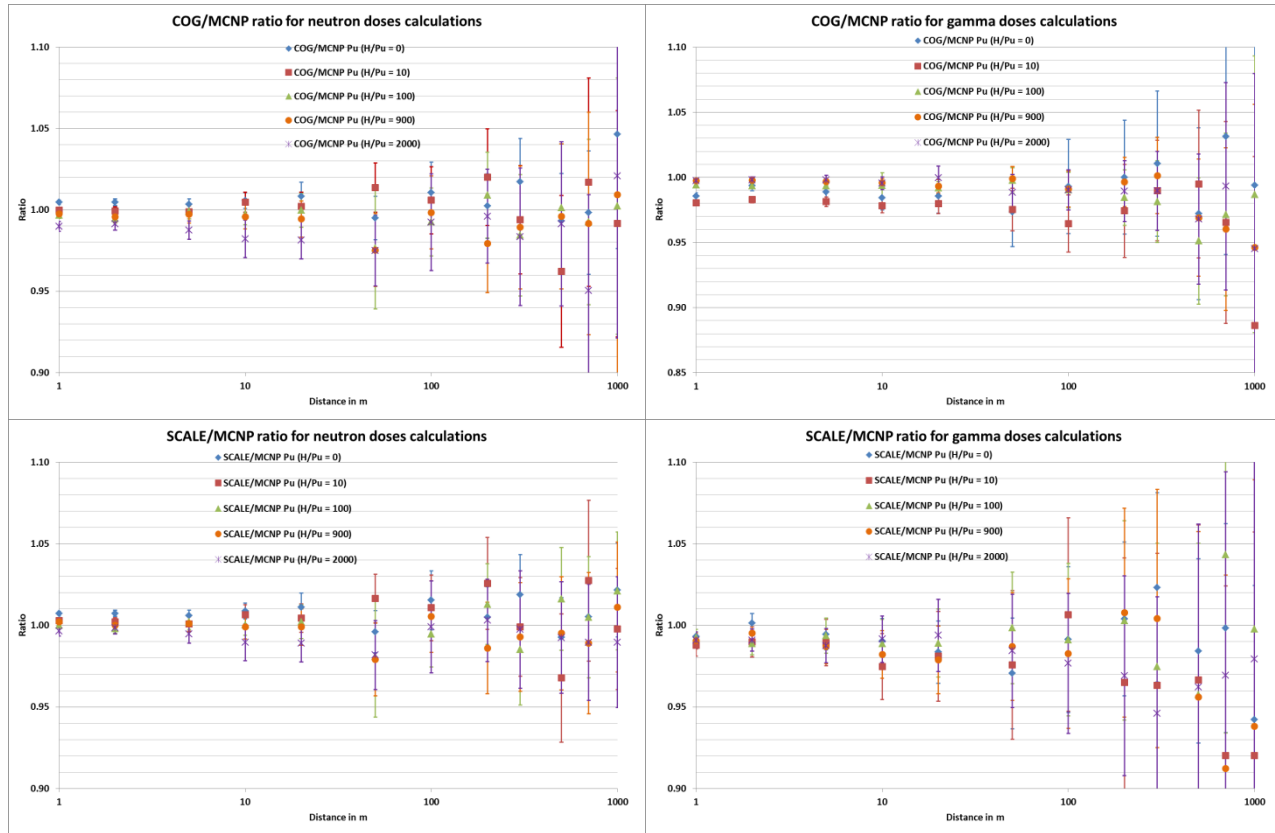


Figure 41. Code to code comparison for the bare plutonium sphere

Figure 42 presents the ratio between neutron and gamma prompt doses calculated with MCNP for bare plutonium system with the Henderson flux-to-dose conversion factor (used in the original slide rule) and the ANSI/HPS N13.3 flux-to-dose conversion factor. It can be seen that the ANSI/HPS N13.3 flux-to-dose conversion factor is more penalizing than the Henderson flux-to-dose conversion factor (at least 20 % for neutron with an increase when the distance increases and about 10 % for gamma independent of the distance). Indeed, the ANSI/HPS N13.3 flux-to-dose conversion factor is always larger than the Henderson flux-to-dose conversion factor with an increasing difference for intermediate and low neutron energies.

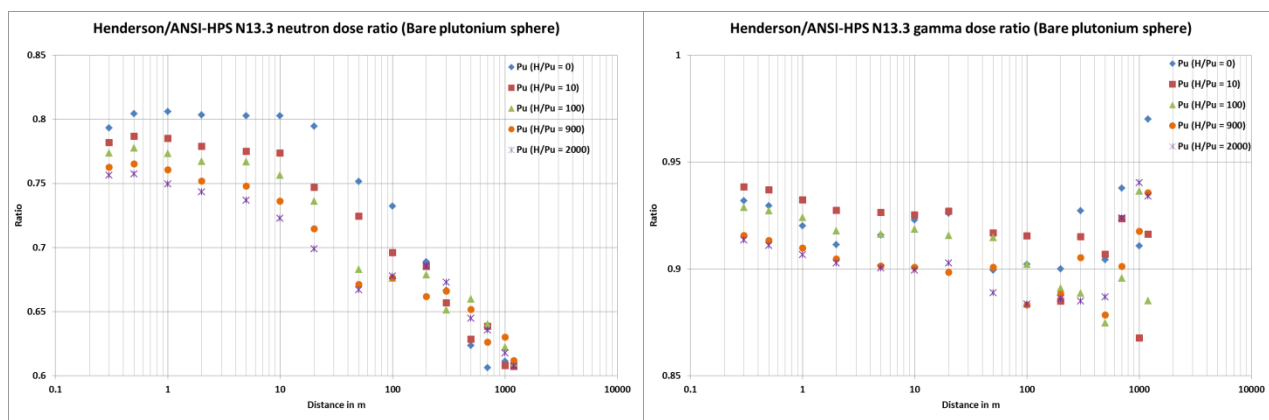


Figure 42. Henderson/ANSI-HPS N13.3 dose ratios for bare plutonium sphere (MCNP)

Figure 43 presents the ANSI/HPS N13.3 and the Henderson flux-to-dose conversion factors for neutrons.

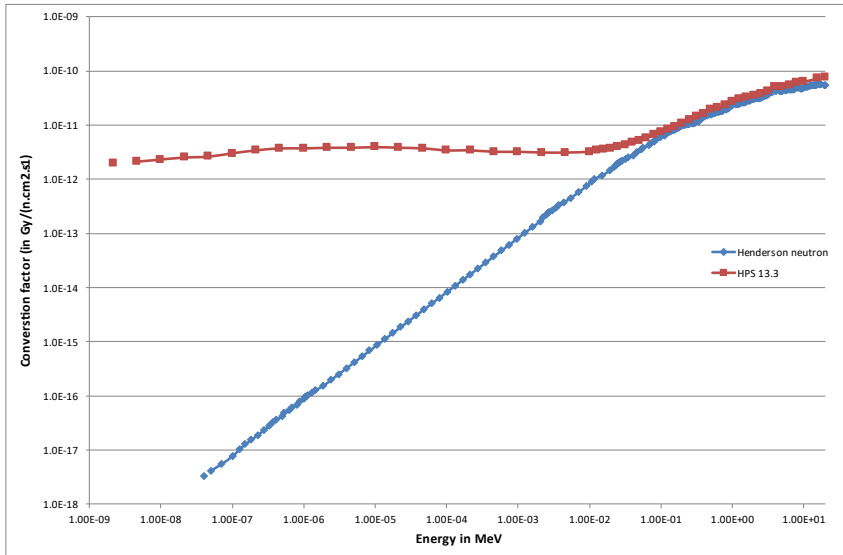


Figure 43. Henderson/ANSI-HPS N13.3 flux-to-dose conversion factors

Figure 44 presents the neutron and gamma prompt doses for the uranium systems (considered in the original slide rule) and the plutonium system calculated with MCNP with the Henderson flux-to-dose conversion factor. These figures show that there are no major differences, in terms of trend, between plutonium and uranium systems. The extreme cases (max/min) for doses are:

- for neutron, plutonium metal and moderated plutonium ($H/Pu = 2000$),
- for prompt gamma, intermediate plutonium system ($H/Pu=100$ or 900) and uranium metal.

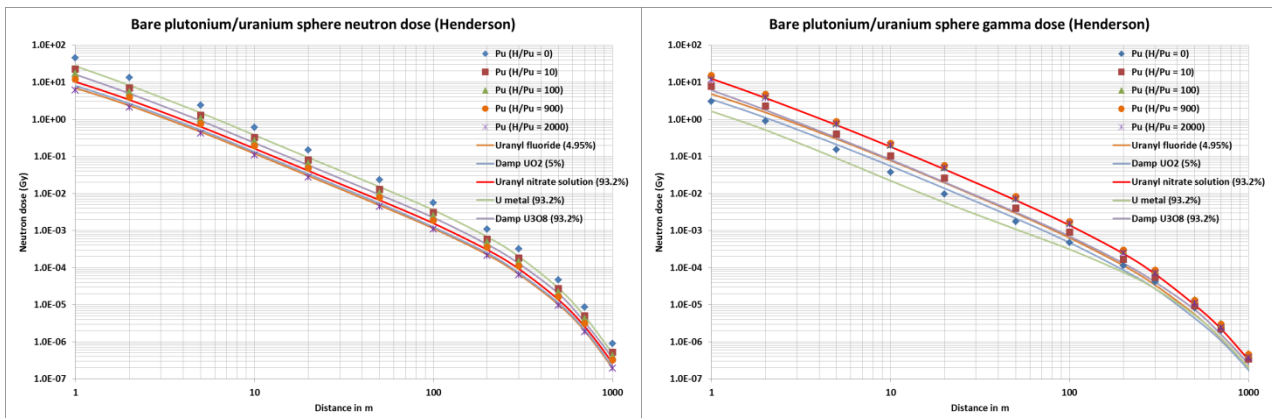


Figure 44. Bare sphere prompt doses using Henderson flux-to-dose conversion factors (MCNP)

It can be seen that, on average for the Henderson flux-to-dose conversion factors, the plutonium metal configuration generates doses 70 % higher than the uranium metal configuration (for both neutrons and prompt gamma). This kind of result shows the interest to update the original slide rule to include plutonium systems.

5.2.2. Bare cylinder calculations

The Figure 45 shows, for neutron and prompt gamma, the ratio between the doses calculated with the critical bare plutonium cylinders (with three different height-to-diameter ratios (0.5, 1 or 2)) and with the critical bare plutonium sphere. The results are shown for two moderation ratios, $H/Pu=0$ and $H/Pu=2000$. The complete dose results are presented in the Appendix 2. The discrepancies between the three cylinders and the sphere are within 30 % and decrease with increasing distance. The solid angle of the various geometries from the detector explains the behavior of the ratio. The ratio tends to approach one for long distances but is not completely reached for gamma

dose for $H/Pu=2\,000$ and a cylinder with a height-to-diameter ratio of 0.5 (but with important relative errors for long distance).

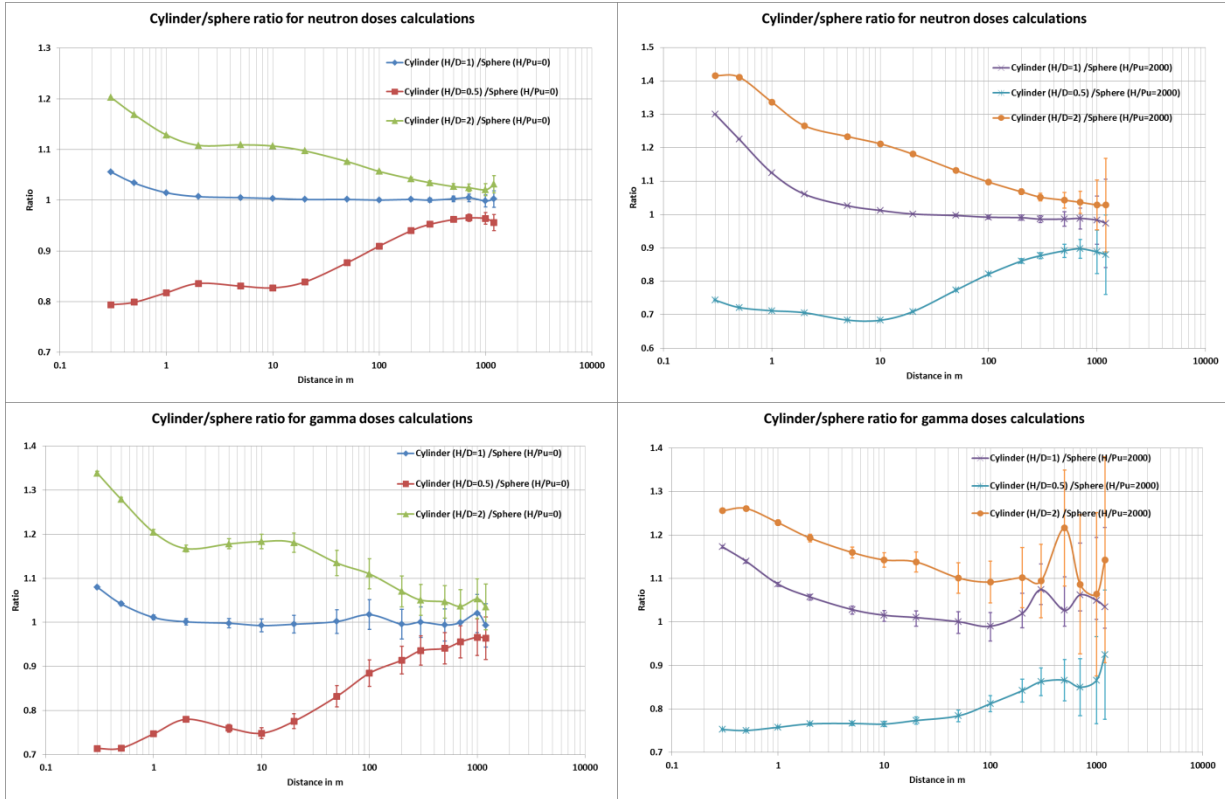


Figure 45. Bare cylinder/sphere dose ratios (SCALE) for $H/Pu=0$ (left) and $H/Pu=2000$ (right)

5.2.3. Reflected sphere calculations

Figure 46 shows, for neutron and prompt gamma, the ratio between the doses calculated with the steel reflected plutonium sphere (with various thicknesses) and with the bare plutonium sphere. The results are shown for two moderation ratios, $H/Pu=0$ and $H/Pu=2000$. The complete dose results are presented in the Appendix 2.

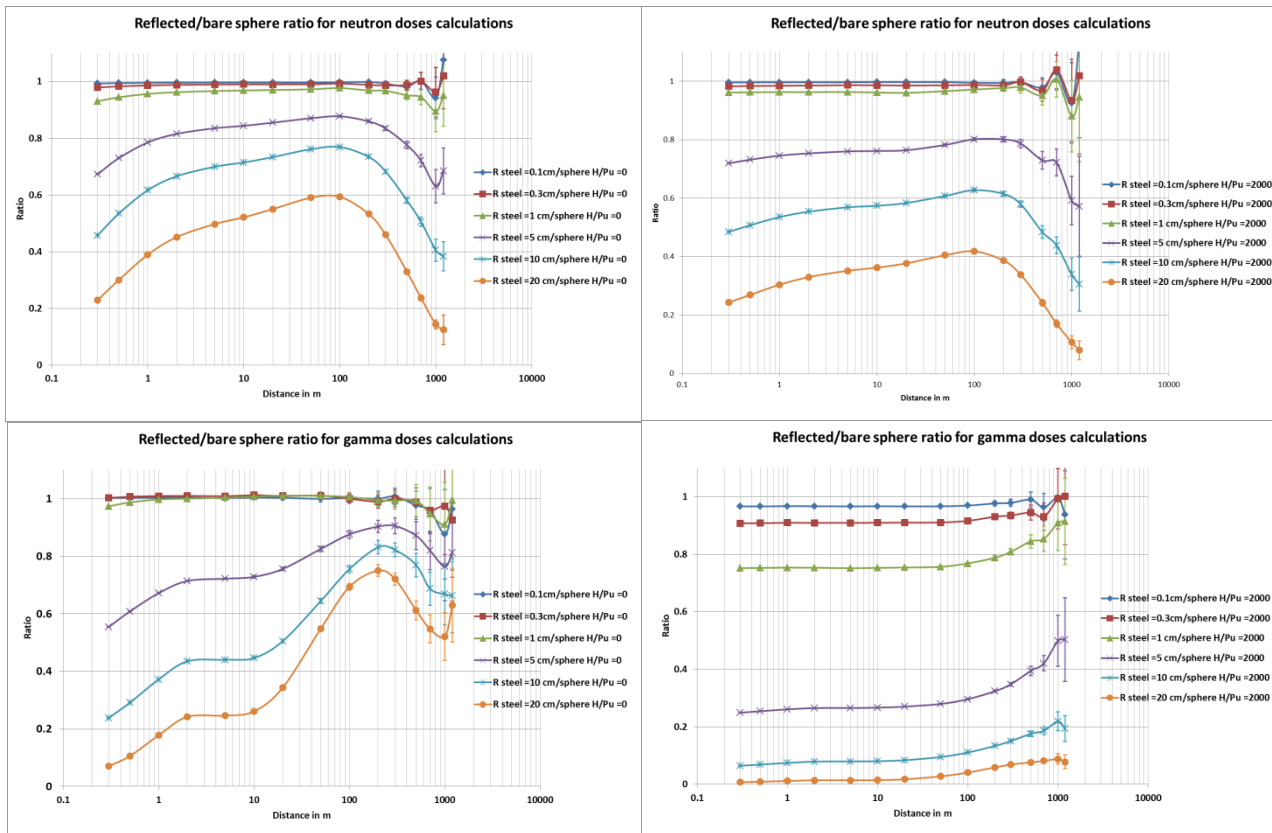


Figure 46. Reflected/bare sphere dose ratios (COG) for $H/Pu=0$ (left) and $H/Pu=2000$ (right)

For these reflector and fissile material configurations, the bare sphere is the most penalizing configuration. The decrease of the size of the critical plutonium sphere (implying less absorption inside the plutonium sphere) does not compensate for the attenuation of the dose due to the reflector. The attenuation effect is not constant with distance and depends on the moderation ratio and the type of incident particle (neutron / gamma). The steel reflector is particularly efficient against the gamma dose for the moderated plutonium ($H/Pu=2000$).

5.3. Delayed fission gamma (DFG)

This section presents and discusses the simulation results obtained for plutonium systems (Pu-239 metal with five moderation ratios) and a comparison with the results of the first phase of the Slide Rule evaluation [14]. DFG dose results are presented in Appendix 5. These simulations and comparisons follow the guidelines detailed in the Phase 4 Task Specification [21].

5.3.1. Configuration overview and assumptions

The time dependent DFG dose rates presented in this report are given in rad/min assuming a criticality accident that generates 10^{17} fissions in 1 μ s (at $t = 0$ s). The expected dose rates for times of 1 s, 5 s, 10 s, 1 min, 5 min, 10 min, 50 min, 100 min, 500 min and 1,000 min after the event are calculated for all five critical systems. For these configurations, only the delayed gamma doses are calculated.

Doses are calculated at 1 m above the ground as a function of distance (between 30 cm and 1,200 m) from the external surface of the source to the center of the detector. By default, the detector geometry is in the shape of a cylindrical shell with a square cross-section of 5 cm x 5 cm, to take advantage of the symmetry of the problem. The center of the detector is also at a height of 1 m above the ground.

Flux-to-dose conversion factors have a significant impact on the final dose and are likely to change in the future. That is why all participants involved used the same response functions to convert the simulated photon fluxes-to-doses, namely Henderson [15], ICRU Report 57 [18], ANSI/HPS N13.3 [20].

5.3.2. DFG dose rates results

At least 750 results¹¹ are calculated to cover all the cases for one conversion factor. Figure 47 presents the DFG dose rates calculated with FISPACT-MCNP only using the ANSI/HPS N13.3 flux-to-dose conversion factor. Calculations have also been performed with the two other conversion factors. In ascending order, ANSI/HPS N13.3 flux-to-dose conversion factor is more penalizing than Henderson one, followed by ICRU-57 (calculated doses about 10 % and 20 % higher respectively). Whatever the case, dose rates decrease by more than 9 orders of magnitude between 30 cm and 1.2 km from the external surface of the source, and by 5 orders of magnitude between 1 s and 1,000 min after the critical event. The difference between the extreme cases goes from a factor 9.3 for short distances to a factor 3.4 for long distances. The lowest dose rate is obtained for the metal plutonium system whereas the highest dose rate is obtained for an intermediate moderation ratio ($H/Pu=100$ or 900).

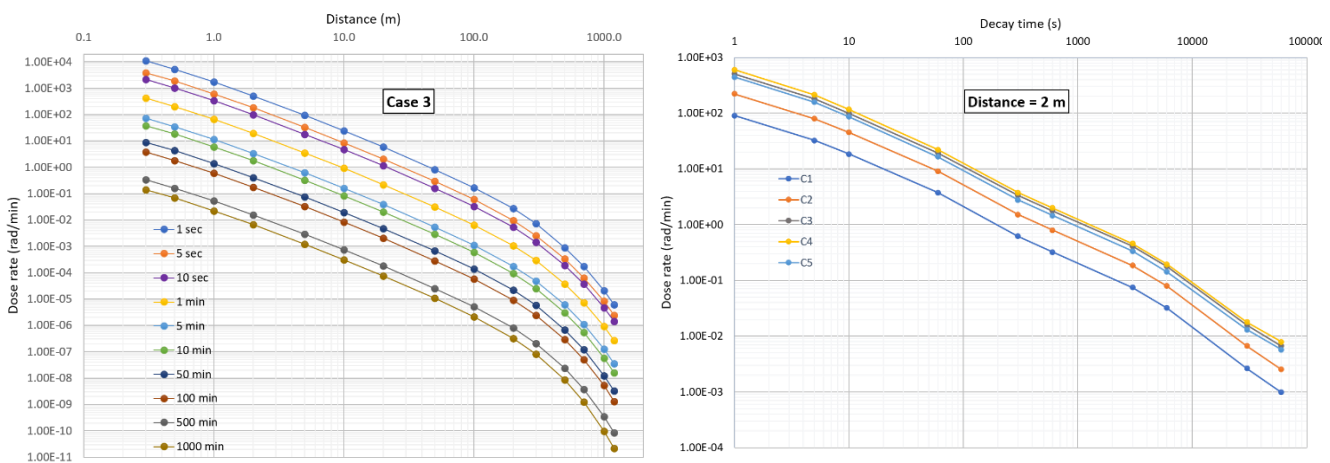


Figure 47. Overview of the ASNR (FISPACT-MCNP) results obtained with HPS N13.3 conversion factor.

Figure 48 presents the DFG dose rate ratio between plutonium metal (case 1) and 93.2 % U-235 enriched uranium metal (obtained from the first phase of the update of the Slide Rule [14] calculated with MCNP and the Henderson flux-to-dose conversion factor. Results show that the DFG dose for Pu system is always higher than U systems. In addition, the DFG dose rate ratio is a slightly higher at short distances and become constant for distances higher than 1 m. It can also be seen that the plutonium metal configuration generates dose rates up to twice higher than the uranium metal configuration (the higher the decay time, the higher the Pu/U ratio). The observed variations of the dose rates from the plutonium configurations compared to the uranium ones are driven by the differences in half-lives of the fission products. These variations show the interest to update the original slide rule with plutonium systems to adapt the emergency response in case of a nuclear criticality accident.

¹¹ 15 distances x 10 decay times x 5 cases (moderation ratios)

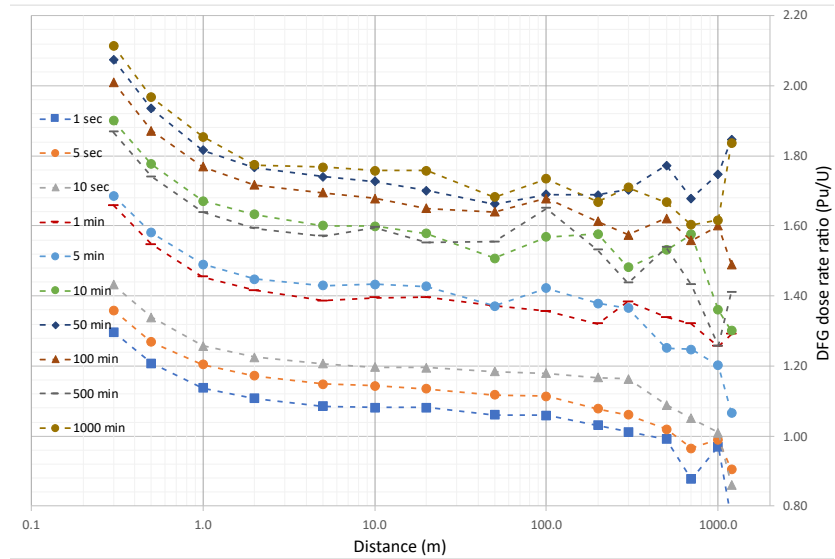


Figure 48 Comparison of DFG dose rates between Pu and U metal ($H/X = 0$).

5.3.3. Code-to-code comparison

Figure 49 and Figure 50 presents code-to-code comparison of DFG dose rates calculated with the ANSI/HPS N13.3 flux-to-dose conversion factors (results are expected to be equivalent with other conversion factors). For a compact visualization, the results' dispersion is displayed on a box-and-whisker graph. The box shows the interquartile range (IQR) which depicts the middle half of the data set. The median is represented by a horizontal bar and the mean by a cross in the box. The whiskers represent the range between the lowest and the highest value, with dots placed past the line edges to indicate outliers. Ratios presented herein are calculated for distances below 300 m, where the relative error due to the codes is lower than 2 %. Each case contains 110 values (11 distances \times 10 decay times).

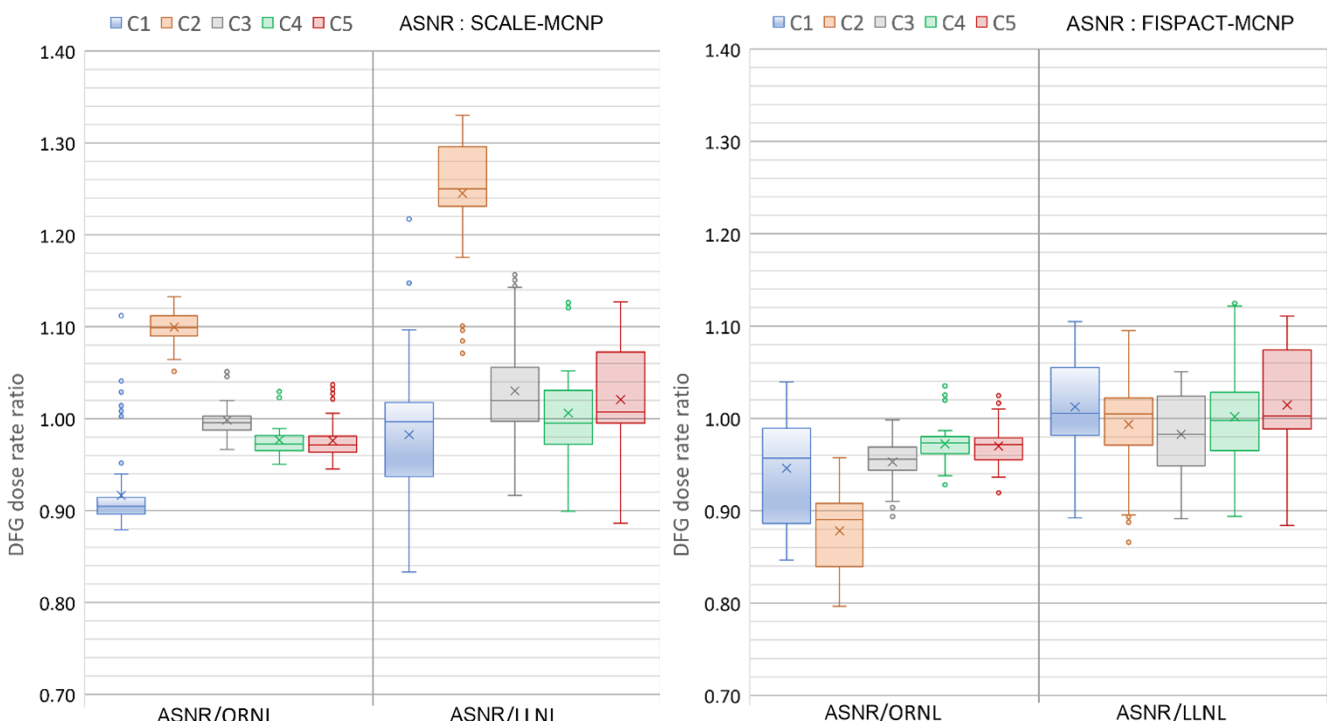


Figure 49 Comparison of ASNR DFG dose rates from two depletion codes with LLNL and ORNL results ($d \leq 300$ m).

While the results of the different codes are relatively close to each other at shorter distances, the discrepancies become more pronounced as the distance increases.

The left-hand side of Figure 49 presents a code-to-code comparison, with ASNR results obtained using SCALE/ORIGEN code for the depletion part (transport code is MCNP for all results). The following observations can be made:

- ASNR/ORNL: the overall distribution is narrowly spread around the mean for all cases. ASNR tends to underestimate ORNL results by approximately 10 % for case 1 and overestimate by 10 % for case 2. For cases 3, 4 and 5 results are in reasonably good agreement, with ratios close to one.
- ASNR/LLNL: except for case 2, a relatively good agreement is observed, although ratios variance is slightly higher. For case 2, ASNR clearly overestimates LLNL results by 20 % to more than 30 %.

The right-hand side of Figure 49 illustrates the similar comparison but with ASNR results obtained using the FISPACT code for depletion calculations:

- ASNR/ORNL: for cases 1 and 2, the distribution is stretched with a trend for ASNR results to underestimate the dose rates calculated by ORNL, with a more pronounced effect for case 2. A relatively good agreement is observed for cases 3, 4 and 5 with a squeezed distribution.
- ASNR/LLNL: for all five cases, a good agreement is observed with discrepancies generally lower than 10 % ($0.95 \leq \text{IQR} \leq 1.07$) and ratios are symmetrically distributed around one.

Upon closer inspection of Figure 48, it becomes apparent that the ASNR/LLNL discrepancies for case 2 significantly decrease. The only change is the use of FISPACT to determine the delayed gamma source. This demonstrates the importance of the choice of depletion code in the accuracy of the results.

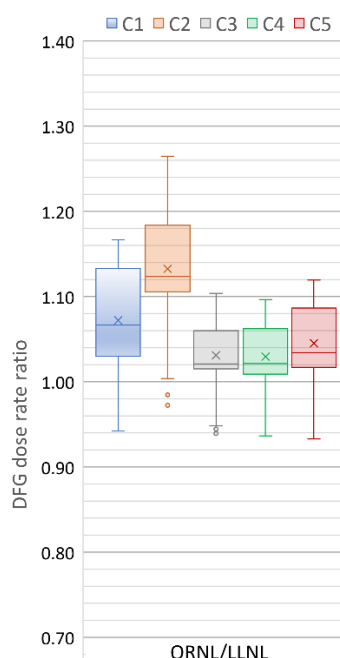


Figure 50 DFG dose rate code-to-code comparison: ORNL vs LLNL results ($d \leq 300 \text{ m}$).

Regarding ORNL results, compared to LLNL (Figure 50), a relatively good agreement is observed for cases 3, 4 and 5. For cases 1 and 2, ORNL tends to overestimate LLNL dose rates with a pronounced tendency for case 2 ($1.0 \leq \text{range} \leq 1.27$ and $1.11 \leq \text{IQR} \leq 1.18$).

The coarse mesh of the multi-group library used by ORIGEN (v7.1-200n47g) to perform the depletion and decay may lack of accuracy in the intermediate energy region where the ^{239}Pu fission cross section is sensitive for case 2. The new very-fine AMPX 1597-group structure (v7.1-1597n) used by ORNL in SCALE 6.3 allows to reduce the gap for this case.

6. FLUX-TO-DOSE CONVERSION FACTORS

Henderson and ANSI/HPS N13.3 flux-to-dose conversion factors were used for the previous studies. These conversion factors allow to produce order of magnitude of prompt and delayed doses. Nevertheless, dose coefficients evolve with time and can show significant differences. In order to expand the area of applicability of the Slide Rule, flux calculations are performed in addition of dose calculations. The energy mesh used for these calculations will allow the Slide Rule user to apply any kind of flux-to-dose conversion factors. The energy mesh used for the flux calculations applies not only to the plutonium configurations described in section 5 but also to the uranium configurations presented in section 4. This approach allows the same methodology to be applied across different fissile media, allowing the Slide Rule user to apply any kind of flux-to-dose conversion factors.

This chapter shows the energy meshes used for the flux calculations. Comparisons are performed between results obtained with these energy meshes and results obtained by a direct calculation.

6.1. Energy mesh for flux calculations

Multiple references, [15] and [20] to [26], were used to create the energy mesh presented in Table 1 and Table 2, the lower boundary of the first group should be zero. This discretization of the flux increases the calculation time because each energy bin must be converged rather than just the total, but it allows one to apply any kind of flux-to-dose conversions factors.

Table 1. Upper bounds in MeV of the neutron energy mesh (from left to right and top to bottom).

1.00E-11	1.00E-09	2.15E-09	4.64E-09	1.00E-08	2.15E-08	2.50E-08	2.60E-08
3.00E-08	4.64E-08	5.00E-08	1.00E-07	2.00E-07	2.15E-07	2.25E-07	3.25E-07
4.15E-07	4.64E-07	5.00E-07	8.00E-07	1.00E-06	1.13E-06	1.30E-06	1.86E-06
2.00E-06	2.15E-06	3.06E-06	4.64E-06	5.00E-06	1.00E-05	1.07E-05	1.10E-05
2.00E-05	2.15E-05	2.90E-05	3.60E-05	4.64E-05	5.00E-05	6.30E-05	1.00E-04
1.01E-04	1.10E-04	2.00E-04	2.15E-04	3.60E-04	4.64E-04	5.00E-04	5.83E-04
6.30E-04	1.00E-03	1.10E-03	2.00E-03	2.15E-03	3.04E-03	3.60E-03	4.64E-03
5.00E-03	6.30E-03	1.00E-02	1.10E-02	1.25E-02	1.50E-02	1.58E-02	2.00E-02
2.51E-02	3.00E-02	3.16E-02	3.60E-02	3.98E-02	5.00E-02	5.01E-02	6.30E-02
7.00E-02	7.94E-02	8.20E-02	8.60E-02	9.00E-02	9.40E-02	9.80E-02	1.00E-01
1.05E-01	1.11E-01	1.15E-01	1.25E-01	1.35E-01	1.45E-01	1.50E-01	1.55E-01
1.58E-01	1.65E-01	1.75E-01	1.85E-01	1.95E-01	2.00E-01	2.10E-01	2.30E-01
2.50E-01	2.51E-01	2.70E-01	2.90E-01	3.00E-01	3.10E-01	3.16E-01	3.30E-01
3.50E-01	3.70E-01	3.90E-01	3.98E-01	4.00E-01	4.08E-01	4.20E-01	4.50E-01
4.60E-01	5.00E-01	5.01E-01	5.40E-01	5.50E-01	5.80E-01	6.00E-01	6.20E-01
6.30E-01	6.60E-01	7.00E-01	7.40E-01	7.80E-01	7.94E-01	8.00E-01	8.20E-01
8.60E-01	9.00E-01	9.07E-01	9.40E-01	9.80E-01	1.00E+00	1.05E+00	1.10E+00
1.15E+00	1.20E+00	1.25E+00	1.30E+00	1.35E+00	1.40E+00	1.43E+00	1.45E+00
1.50E+00	1.55E+00	1.58E+00	1.60E+00	1.65E+00	1.70E+00	1.75E+00	1.80E+00

1.83E+00	1.85E+00	1.90E+00	1.95E+00	2.00E+00	2.10E+00	2.20E+00	2.30E+00
2.40E+00	2.50E+00	2.60E+00	2.70E+00	2.80E+00	2.90E+00	3.00E+00	3.10E+00
3.15E+00	3.20E+00	3.30E+00	3.40E+00	3.50E+00	3.60E+00	3.70E+00	3.75E+00
3.80E+00	3.90E+00	4.00E+00	4.10E+00	4.20E+00	4.30E+00	4.50E+00	4.60E+00
4.70E+00	4.80E+00	4.90E+00	5.00E+00	5.10E+00	5.20E+00	5.30E+00	5.40E+00
5.50E+00	5.60E+00	5.80E+00	6.00E+00	6.20E+00	6.30E+00	6.40E+00	6.50E+00
6.60E+00	6.70E+00	7.00E+00	7.30E+00	7.40E+00	7.50E+00	7.70E+00	7.80E+00
7.94E+00	8.00E+00	8.20E+00	8.30E+00	8.50E+00	8.60E+00	9.00E+00	9.40E+00
9.80E+00	1.00E+01	1.05E+01	1.10E+01	1.15E+01	1.20E+01	1.25E+01	1.30E+01
1.35E+01	1.40E+01	1.45E+01	1.50E+01	1.60E+01	1.70E+01	1.80E+01	2.00E+01
2.20E+01	2.40E+01	2.60E+01	2.80E+01	3.00E+01	3.50E+01	4.00E+01	4.50E+01
5.00E+01	5.50E+01	6.00E+01	6.50E+01	7.00E+01	7.50E+01	8.00E+01	8.50E+01
9.00E+01	9.50E+01	1.00E+02	1.10E+02	1.20E+02	1.25E+02	1.30E+02	1.40E+02
1.50E+02	1.75E+02	1.80E+02	2.01E+02				

Table 2. Upper bounds in MeV of the gamma energy mesh (from left to right and top to bottom)

1.00E-02	1.25E-02	1.50E-02	1.75E-02	2.00E-02	2.50E-02	3.00E-02	4.00E-02
4.50E-02	5.00E-02	6.00E-02	7.00E-02	8.00E-02	1.00E-01	1.25E-01	1.50E-01
2.00E-01	2.50E-01	3.00E-01	3.50E-01	4.00E-01	4.50E-01	5.00E-01	5.50E-01
6.00E-01	6.50E-01	7.00E-01	8.00E-01	1.00E+00	1.10E+00	1.20E+00	1.33E+00
1.40E+00	1.50E+00	1.66E+00	1.80E+00	2.00E+00	2.20E+00	2.50E+00	2.60E+00
2.80E+00	3.00E+00	3.25E+00	3.50E+00	3.75E+00	4.00E+00	4.25E+00	4.50E+00
4.75E+00	5.00E+00	5.25E+00	5.50E+00	5.75E+00	6.00E+00	6.25E+00	6.50E+00
6.75E+00	7.50E+00	8.00E+00	8.50E+00	9.00E+00	9.50E+00	1.00E+01	1.10E+01
1.30E+01	1.50E+01	2.00E+01					

6.2. Application of a flux-to-dose conversions factors

The energy mesh presented above enables using any kind of flux-to-dose conversion factors. Those factors can be defined by histograms or values that can be interpolated. This section compares results from a direct calculation and a ‘two step’ calculation where the flux is calculated first (using the energy mesh defined above) and the flux-to-dose conversion factors are applied in a second step. These calculations are performed using MCNP 6.1 for the first case bare plutonium system.

6.2.1. Comparisons for the neutron doses

Flux-to-dose conversion factors from seven references (see Table 3) are used in this section to perform comparisons with the two step calculations. Table 4 presents the ratios of the total neutron dose calculated using the energy mesh with a ‘two-step’ calculation and a direct calculation. Throughout the rest of the document, the

designations presented in Table 3 are used. Responses with an odd number are used for neutron flux and responses with an even number are used for gamma flux.

Table 3. Designations of the different flux-to-dose conversion factors

Resp 1 / Resp 2	Air kerma – [22]
Resp 3 / Resp 4	Tissue kerma in air – [23]
Resp 5 / Resp 6	Henderson absorbed dose – [15]
Resp 7 / Resp 8	ANSI/HPS N13.3 – [20]
Resp 9 / Resp 10	ICRU 57 ambient dose equivalent – [24]
Resp 11 / Resp 12	ICRP 74 ambient dose equivalent – [25]
Resp 13 / Resp 14	ICRU 57 effective dose – [24]
Resp 15 / Resp 16	ICRP 116 effective dose – [26]

Table 4. Ratios and relative errors of the neutron prompt dose calculated using the energy mesh with a ‘two-step’ calculation and a direct calculation

dist (m)	resp 1	resp 3	resp 5	resp 7	resp 9	resp 11	resp 13	resp 15
0.3	0.98	0.04%	0.99	0.03%	1.00	0.01%	0.99	0.01%
0.5	0.99	0.06%	0.99	0.06%	1.00	0.01%	0.99	0.01%
1	0.99	0.09%	0.99	0.09%	1.00	0.01%	0.99	0.01%
2	0.99	0.14%	0.99	0.14%	1.00	0.02%	0.99	0.02%
5	0.99	0.22%	0.99	0.21%	1.00	0.03%	0.99	0.03%
10	1.00	0.36%	0.99	0.35%	1.00	0.04%	1.00	0.04%
20	1.00	0.50%	0.99	0.48%	1.00	0.05%	0.99	0.05%
50	1.02	0.98%	1.00	0.92%	1.01	0.08%	1.00	0.92%
100	1.02	1.26%	0.99	1.15%	1.01	0.11%	0.99	1.15%
200	1.02	1.12%	1.00	0.99%	1.02	0.16%	1.00	0.98%
300	1.01	1.25%	1.00	1.12%	1.02	0.21%	1.00	1.11%
500	1.06	1.21%	1.00	1.10%	1.02	0.33%	1.00	1.09%
700	1.04	1.13%	0.99	1.09%	1.02	0.48%	0.99	1.06%
1000	1.05	1.14%	0.97	1.21%	1.00	0.79%	0.98	1.16%
1200	1.03	1.12%	0.96	1.27%	0.99	1.11%	0.97	0.97

The discrepancies observed for these calculations are low enough to prove that the neutron energy mesh is well defined to performed dose calculations.

6.2.2. Comparisons for the gamma doses

The comparisons performed in the previous section are repeated for gamma doses. Table 5 shows the ratios calculated for the first bare plutonium system.

Table 5. Ratios and relative errors of the gamma prompt dose calculated using the energy mesh with a ‘two-step’ calculation and a direct calculation

dist (m)	resp 1		resp 3		resp 5		resp 7		resp 9		resp 11		resp 13		resp 15	
0.3	1.00	0.06%	1.00	0.06%	1.02	0.05%	1.00	0.06%	1.00	0.06%	1.00	0.06%	1.00	0.06%	1.00	0.06%
0.5	1.00	0.10%	1.00	0.10%	1.02	0.06%	1.00	0.10%	1.00	0.10%	1.00	0.10%	1.00	0.10%	1.00	0.10%
1	1.00	0.16%	1.00	0.16%	1.02	0.11%	1.01	0.17%	1.00	0.16%	1.00	0.16%	1.00	0.16%	1.00	0.16%
2	1.00	0.24%	1.00	0.24%	1.03	0.16%	1.01	0.25%	1.00	0.24%	1.00	0.24%	1.00	0.24%	1.00	0.24%
5	1.00	0.41%	1.00	0.41%	1.02	0.26%	1.00	0.42%	1.00	0.40%	1.00	0.40%	1.00	0.41%	1.00	0.40%
10	1.00	0.76%	1.00	0.77%	1.02	0.51%	1.01	0.74%	1.00	0.73%	1.00	0.73%	1.00	0.72%	1.00	0.72%
20	1.01	0.84%	1.00	0.85%	1.02	0.56%	1.01	0.85%	0.99	0.85%	0.99	0.85%	0.99	0.87%	0.99	0.86%
50	1.00	1.77%	1.00	1.74%	1.02	1.12%	1.00	1.81%	1.01	1.71%	1.00	1.69%	1.01	1.69%	1.00	1.69%
100	1.02	2.34%	1.00	2.35%	1.04	1.41%	1.02	2.51%	1.00	2.33%	1.01	2.28%	1.00	2.35%	1.01	2.28%
200	0.98	2.79%	0.98	2.80%	1.03	1.84%	1.02	2.89%	1.01	2.72%	1.01	2.72%	1.01	2.73%	1.01	2.78%
300	1.01	3.11%	1.02	3.10%	1.05	1.89%	1.03	3.47%	1.03	3.00%	1.03	3.04%	1.03	3.20%	1.03	3.17%
500	1.02	3.28%	1.01	3.29%	1.04	2.04%	1.01	3.41%	1.04	3.15%	1.04	3.16%	1.04	3.20%	1.04	3.18%
700	1.03	3.80%	1.02	3.88%	1.08	2.30%	1.06	3.94%	1.06	3.78%	1.05	3.60%	1.06	3.60%	1.05	3.58%
1000	1.03	4.33%	1.06	4.62%	1.03	2.74%	0.99	4.81%	1.00	4.25%	1.03	4.23%	1.00	4.48%	1.03	4.33%

The discrepancies observed for these calculations are low enough to prove that the gamma energy mesh is well defined to performed dose calculations.

7. CONCLUSIONS AND PERSPECTIVES

This report presents an in-depth analysis conducted by ASNR, AWE, LLNL, and ORNL to update the Nuclear Criticality Slide Rule for emergency response to nuclear criticality accidents. The study focused on:

- Developing a calculation scheme applied to five fissile media included in the "Slide Rule",
- Extending the scope of the original "Slide Rule" to include plutonium systems, enhancing its applicability to a broader range of criticality scenarios,
- Performing comparisons between Monte Carlo codes (MCNP, SCALE, and COG) to validate the consistency and reliability of different computational approaches,
- Conducting sensitivity studies to evaluate the impact of different parameters such as air humidity and ground composition on dose calculations,
- Analyzing configurations involving shielding screens to understand their effectiveness in dose attenuation during criticality incidents,
- Evaluating differences between various flux-to-dose conversion factors, such as those from ANSI/HPS N13.3 and Henderson, while also using a universal energy mesh that allows the application of any flux-to-dose conversion factor.

The updated Slide Rule aims to enhance real-time response capabilities by leveraging state-of-the-art computational tools and broadening the range of criticality scenarios considered. The findings of this report not only highlight the necessity of updating the original 1997 Slide Rule for prompt dose estimates but also highlight the necessity of updates when addressing new configurations, especially those involving plutonium. The inclusion of modern tools has enabled more precise estimates of prompt and delayed doses, thereby providing an opportunity to improve protective measures and emergency response strategies.

Ongoing developments include the creation of a Slide Rule application for handheld devices, providing emergency responders with rapid access to critical data. Future work will include extended sensitivity studies on plutonium systems to further refine the Slide Rule's applicability and accuracy.

This initiative not only updates a critical tool in nuclear safety but also strengthens international collaboration, ultimately aiming to better equip emergency response teams in managing criticality incidents and minimizing their potential consequences.

REFERENCES

- [1] B. L. Broadhead et al., "An Updated Nuclear Criticality Slide Rule: Technical Basis," Report NUREG/CR-6504 Vol. 1 ORNL/TM-13322/V1, (1997).
- [2] C. M. Hopper, and B. L. Broadhead, "An Updated Nuclear Criticality Slide Rule: Functional Slide Rule," Report NUREG/CR-65[404, Vol. 2 ORNL/TM-13322/V2, (1998).
- [3] Fiches Accident-Type, IPSN internal report, (2000).
- [4] M. Duluc et al., "Update of the Nuclear Criticality Slide Rule for the Emergency Response to a Nuclear Criticality Accident," ICRS 13 RPSD 2016 conference, October 3-6, 2016 Paris, France (2016).
- [5] M. Duluc et al., "Introduction of plutonium systems to the nuclear criticality Slide Rule," ANS NCSD 2017 conference, September 10-15, 2017, Carlsbad, NM USA (2017).
- [6] NCSP website, <http://ncsp.llnl.gov/>
- [7] C.J. Werner et al., "MCNP Version 6.2 Release Note", LA-UR-18-20808, LANL, Los Alamos, NM US (2018).
- [8] B. C. Kiedrowski, "MCNP6 for criticality accident alarm systems – A Primer," LA-UR-12-25545 (2012).
- [9] M. Troisne, "Révision du document Slide Rule. Calcul des configurations initiales", Report IRSN/PSN-EXP/SNC/2017-016 (2017).
- [10] S. W. Mosher et al., "ADVANTG—An Automated Variance Reduction Parameter Generator," ORNL/TM-2013/416 Rev. 1 (2015).
- [11] W. A. Wieselquist, R. A. Lefebvre, and M. A. Jessee, Eds., "SCALE Code System", ORNL/TM-2005/39, Version 6.2.4, Oak Ridge National Laboratory, Oak Ridge, TN (2020).
- [12] J-Ch. Sublet et al., "FISPACT-II: An Advanced Simulation System for Activation, Transmutation and Material Modelling", Nuclear Data Sheets, Volume 139, pp. 77-137 (2017).
- [13] "COG: A Multiparticle Monte Carlo Code Transport Code", Version 11.1, CCC-829, Released by Radiation Safety Information Computational Center (2015).
- [14] "Update of the nuclear criticality Slide Rule calculations – Initial configurations", Phase 1 Task Specification (2015).
- [15] B. J. Henderson, "Conversion of Neutron or Gamma-Ray Flux to Absorbed Dose", XDC 59-8-179 (1959).
- [16] I. Gauld, "Validation of ORIGEN-S decay heat predictions for LOCA analysis," PHYSOR 2006, Vancouver, BC, Canada, September 10-14, (2006).
- [17] "Update of the nuclear criticality Slide Rule calculations – Sensitivity studies", Phase 3 Task Specification (2017).
- [18] "Conversion Coefficients for use in Radiological Protection against External Radiation", ICRU Report 57 (1998).
- [19] "Update of the nuclear criticality Slide Rule calculations – Plutonium configurations", Phase 2 Task Specification (2017).
- [20] "Dosimetry for Criticality Accidents", ANSI/HPS Standard N13.3, 2013 Edition (2013).
- [21] "Update of the nuclear criticality Slide Rule calculations – Plutonium configurations – Delayed gamma", Phase 4 Task Specification (2020).
- [22] "Tissue Substitutes in Radiation Dosimetry and Measurement", ICRP Report 44 (1989)
- [23] "Dosimetry for Criticality Accident", IAEA 211 (1982)
- [24] "Conversion Coefficients for use in Radiological Protection Against External Radiation", ICRU Report 57 (1998)
- [25] "Conversion Coefficients for use in Radiological Protection Against External Radiation", ICRP publication 74 (1996), ISSN 0146-6453

- [26] "Conversion Coefficients for Radiological Protection Quantities for External Radiation Exposures", ICRP Publication 116 (2010), ISBN 978-1-4557-2858-9



Adresse du siège social :
15 rue Louis Lejeune - 92120 Montrouge

Adresse postale :
BP 17 - 92262 Fontenay-aux-Roses cedex

Courriel : asnrcourrier@asnrf.fr

TÉLÉPHONE
+33 (0)1 58 35 88 88

SITE INTERNET
www.asnr.fr